



Berberine-enriched copper oxide nano formulation synthesized using *Solanum torvum*: A strategic advancement in lung cancer therapy and wound healing

Manju Bargavi Sakthivel¹, Prabhavathy Devi Narayanan Dass^{1*}, Tharani Munusamy^{2*}, Nalini Devarajan², Pavithra Amritkumar², Suresh Malchi², Naresh Kumar Kodiganti², Karunanidhi Kannappan²

¹Department of Nutrition and Dietetics, Faculty of Humanities and Science, Meenakshi Academy of Higher Education and Research, Chennai, India.

²Department of Research, Meenakshi Academy of Higher Education and Research, Chennai, India.

ARTICLE HISTORY

Received on: 11/01/2025
Accepted on: 03/04/2025
Available Online: 05/05/2025

Key words:

Berberine, *Solanum torvum*, copper oxide nano formulation, anti-cancer activity, Lung cancer cell, A549 cell lines.

ABSTRACT

This study aimed to synthesize a Berberine conjugated with Copper Oxide Nano Formulation (BBR-CuONPs) by using *Solanum torvum* for lung cancer therapy. The BBR-CuONPs were evaluated for their anticancer activity by assessing cell movement and proliferation in non-small cell lung cancer cell lines (A549). Berberine chloride and copper sulfate were utilized to prepare the BBR-CuONPs, while *S. torvum* extract acted as a reducing agent for green synthesis. The characterization of the BBR-CuONPs was carried out using UV-visible spectrophotometry, Fourier-transform infrared spectroscopy (FTIR), and transmission electron microscopy (TEM). The UV-visible spectra confirmed the synthesis of BBR-CuONPs, showing characteristic absorption peaks. FTIR analysis revealed functional groups indicative of interactions between CuONPs and berberine, suggesting their potential synergistic effects. TEM images showed the nanoparticles had an average size ranging from 10 to 50 nm. The anti-cancer activity (MTT assay) demonstrated a dose-dependent inhibition of cell viability, with a calculated IC_{50} value of $32.35 \pm 2 \mu\text{g}$, indicating that it has an effective cytotoxic activity with controlled and sustained drug release for a longer time than compared with berberine and copper oxide nanoparticles alone. The BBR-CuONPs, in normal human embryonic kidney (HEK) cells, were observed that higher cell viability at 10 $\mu\text{g/ml}$ (98%) and less cytotoxicity effect at 100 $\mu\text{g/ml}$ (2%) inhibition even in higher concentration. The wound healing assay confirmed the suppression of A549 cell migration, with 10 $\mu\text{g/ml}$ (24–48 hours) at lower concentrations of the nano formulation showing stronger inhibition. This study suggests that the BBR- CuONPs derived from *S. torvum* exhibit promising anticancer and wound-healing properties, supporting further *in vivo* investigation into their therapeutic potential.

INTRODUCTION

Lung cancer: prevalence, impact, and treatment challenges

According to the research findings, Lung cancer contributes to major causes of cancer deaths worldwide (World Health Organization). In the year 2022, it was reported that almost 2.5 million people were detected and 1.8 million people died from the disease. When compared to colorectal cancer, lung cancer causes more than twice the causes of cancer death. The primary risk factor for causing lung cancer is smoking and it is responsible for about 85% of all cases. The secondary causes include contamination exposure from second-hand smokers,

*Corresponding Author

Prabhavathy Devi Narayanan Dass, Department of Nutrition and Dietetics, Faculty of Humanities and Science, Meenakshi Academy of Higher Education and Research, Chennai, India.
E-mail: prabhavathy_devi@yahoo.com;

Tharani Munusamy, Department of Research, Meenakshi Academy of Higher Education and Research, Chennai, India.
E-mail: Tharanimano@gmail.com

air pollution, welding fumes, and diesel engine exhaustion [1]. According to the histology of cancer cells, lung cancer can be classified into two types: small-cell lung cancer and non-small-cell lung cancer (NSCLC). Among that, approximately 85%–90% of the lung cancer is NSCLC [2]. The most common symptoms include a long-term cough that does not go away, chest pain, shortness of breath, fatigue, recurring lung infection, and weight loss for unknown reasons.

To prevent lung cancer, people must avoid smoking tobacco so that second-hand tobacco smokers can also benefit. If treatment started early as soon as the diagnosis has been identified the metastasis of the lung cancer can be prevented from becoming worse condition and metastasis. The prevention of lung cancer can be classified into primary and secondary prevention. The primary aim is to reduce the initial occurrence of a disease and promote a healthy life. Secondary prevention includes the screening methods of cancer both physical and biological aspects to detect the diseases in an earlier stage to increase the chances for successful treatment and improve outcomes. The primary screening method used for lung cancer is low-dose computed tomography [1].

The better choice for the most appropriate treatment depends on the functional assessment of the patient and the stage of the disease. Surgery is the standard treatment of lung cancer, however, in the case of metastatic and advanced stages, it might not be appropriate [3]. All the traditional chemotherapeutic drugs have the same limitations, which include non-specific targeting, low bioavailability, and the development of drug resistance, thus limiting their efficacy in cancer treatment [2].

Nanoparticles act as an enhanced drug delivery systems for targeted cancer therapy

However, recent approaches such as targeted therapy and immunotherapy have transformed the management strategy for the treatment of lung cancer [4]. This research focuses on the nano-based formulation for the targeted therapy. Nanoparticles (NPs), defined as synthetic particles with diameters less than 100 nm, are typically derived from polymers, lipids, or metals like gold. These nanoscale particles have demonstrated significant utility across various medical applications, ranging from diagnostic tools to therapeutic interventions in cancer [5]. Due to their size, which closely mimics that of many biological molecules and structures, NPs exhibit unique functional properties that are advantageous for cancer research in both *in vivo* and *in vitro* settings [6]. When nanoparticles are combined with biodegradable carriers they can be safely loaded with therapeutic agents, enabling targeted local drug delivery with the added benefit of sustained release [7]. Their unique properties allow them to enter the body and circulate through the bloodstream, offering minimal invasiveness and enhanced bioavailability [8].

Targeted techniques and specific ligands used for drug delivery system

Recently, Nanomedicine has been used to treat cancer by focusing on drug delivery and improving therapeutic effects with minimal effects on normal cells [9]. Nanoparticles are used

for lung cancer treatment and can be divided into two forms, organic and inorganic nanoparticles. The organic nanoparticles can be further divided into 1) liposome and phospholipid-like biofilm nano particles, 2) solid lipid nanoparticles, 3) lipid carriers mixed with solid lipid and liquid lipids, 4) polymeric nanoparticles composed of polymers, 5) polymeric micelles-colloidal nanoparticles composed of amphiphilic block copolymers, and 6) dendrimer-highly branched, symmetrical, radiating nanoparticles. Inorganic NPs are classified into three types: 1) magnetic NPs-superparamagnetic materials, 2) carbon nanotubes, and 3) quantum dots-colloidal nanoparticles [10].

There are two targeting techniques: active and passive. Passive technique covers three aspects. 1. Uses of tumors for enhancing the penetration and retention effect for the nanoparticle to induce and accumulate in tumor tissue, which does not work in humans [11]. The second aspect is to use the acidic microenvironment of tumors to limit the action of nanoparticles to acidic conditions [12]. Thirdly, tumor cells can be used to carry additional negative charges, therefore nanoparticles contain positively charged [13].

Active targeting techniques involving to modify the surface of nanoparticles with specific ligands that bind to overexpressed receptors on lung cancer cells or blood vessels, nanoparticles are used for targeting more precisely than passive techniques. Additionally, certain receptors and ligands have been shown to facilitate cell endocytosis and inhibit tumor multi-drug resistance [14]. Antibodies, aptamers, fragments, or peptides are frequently used as ligands.

Recent advances in immunotherapy, specifically targeting immune checkpoints such as programmed cell death protein 1 and programmed death-ligand 1, have shown promise in improving treatment outcomes, and chemotherapy continues to be the most commonly utilized therapeutic approach for NSCLC [15,16]. In many cases, in over 50% of cancers, the tumor suppressor protein p53 is mutated and plays a pivotal role in tumorigenesis and cancer progression. The mutation of p53 in tumors showed resistance to conventional therapies [17,18]. Therefore, this research focused on identifying novel therapeutic drugs capable of exhibiting anticancer effects through p53-independent mechanisms.

Copper oxide nanoparticles via green synthesis

Traditional methods for producing nanomaterials are efficient but it has an impact on environmental and economic drawbacks, including toxic chemicals, energy, and bio-waste. These challenges limit their commercial scalability and clinical use due to issues of biocompatibility and toxicity. In contrast, green synthesis of nanoparticles offers a more sustainable, cost-effective, and biocompatible alternative, addressing these concerns while minimizing environmental impact. Green synthesis being environmentally friendly has beneficial effects such as reduced toxicity, cost-effectiveness, improved biocompatibility, and better size control have made it a preferred method for producing nanomaterials compared to traditional physical and chemical approaches [19].

Metal oxide NPs attract significant attention due to their remarkable properties, including those of copper, zinc,

titanium, iron, and tin [20,21]. Copper oxide (CuO) NPs are gaining attention due to their cost-effectiveness and promising applications, particularly as an alternative to noble metal oxides [22]. As semiconductor NPs, copper oxide nanoparticles (CuONPs) have shown potential in photoconductive and photothermal applications [23]. They are highly susceptible to oxidation, especially in the presence of air and water, but remain stable at temperatures below 200°C. Copper oxide NPs also exhibit strong antimicrobial properties, effectively combating bacteria, fungi, viruses, and algae, thanks to their increased surface area.

Abraham *et al.* [24] current evidence suggests that rich in phytochemicals and bioactive compounds, significantly promote the growth of CuONPs and enhance their biological properties, particularly their anticancer activity against A549 cell lines. This evidence underscores the potential of CuONPs as a promising therapeutic agent in cancer treatment [25]. Nanoparticle synthesis by using biological methods including plant extract, microbes, and marine sources is helpful in many aspects such as biosafety, cost-efficiency, minute toxicity levels, and socio-economic advantages [26].

Tumor biomarkers and imaging techniques used in the copper nanoparticles

The vivo study has been conducted in the copper nanoparticles and has shown significant potential in the treatment of cancer due to their ability to induce tumor cell death through mechanisms such as apoptosis, paraptosis, inhibition of angiogenesis, and cuproptosis (targeting cell copper death mechanism). Therefore, these nanoparticles are used for the investigation of advanced therapeutic approaches such as chemo dynamic therapy, phototherapy, hyperthermia, and immunotherapy, thus making it a dual purpose for diagnostic and applications. However, tumor cells require a higher quantity of copper for metabolism but excess copper would lead to adverse effects like tumor growth and metastasis which become more challenging in clinical aspects. It is essential to evaluate their mechanism in-depth and address their limitations in the future [27].

Role of *Solanum Torvum* in copper oxide nanoparticle synthesis

Solanum torvum, commonly known as turkey berry, is a medicinal plant belonging to the Solanaceae family, found across tropical regions of Africa, Asia, and South America. It is widely utilized in folk medicine and as food, particularly in tropical and subtropical countries, *S. torvum* is recognized for its diverse pharmacological properties. The plant contains various bioactive metabolites, including steroid glycosides, saponins, flavonoids, vitamins, and alkaloids, which contribute to its medicinal value. Traditionally, it has been used to treat diseases such as fever, wounds, tooth decay, reproductive issues, cardiovascular and hypertension. Some of the research has found out it if antioxidant, immunomodulatory, and nephroprotective activities, further supporting its therapeutic applications. Copper being an antibacterial agent possesses low toxic effects on human cells. In the field of medicine, copper

oxide nanoparticles are used as a topical application for burns and other injuries [28].

Solanum torvum fruits are rich in diverse phytochemicals, including alkaloids, flavonoids, saponins, glycosides, tannins, phenols, and sugars, along with essential nutrients such as vitamin C, folate, potassium, and fiber, making them valuable for both medicinal and nutritional applications [29]. These bioactive compounds support plant growth, reproduction, and defense by acting as antifeedants and antipathogens [30]. Additionally, alkaloids, flavonoids, and saponins exhibit significant therapeutic potential, particularly in cancer prevention and treatment, by regulating gene expression and signal transduction pathways. As chemo-preventive agents, they help constrain, reverse, or delay tumorigenesis, with their molecular mechanisms often overlapping with those involved in cancer therapy [31]. Moreover, these phytochemicals serve as natural reducing and stabilizing agents in the green synthesis of nanoparticles, enhancing their biomedical applications, including antimicrobial, anticancer, and wound-healing properties [32].

Berberine: a promising anticancer agent

Berberine, an iso-quinoline alkaloid, is primarily derived from the roots, stems, bark, and rhizomes of plants like *Berberis*, *Phellodendron amurense*, *Coptis chinensis*, and *Hydrastis canadensis* [33]. These plants have been used in Chinese medicine for over 2,000 years to treat various diseases [34]. Recent researchers have identified berberine as the key pharmacologically active compound, recognized for its broad therapeutic properties, including antimicrobial, antioxidant, anti-inflammatory, antidiabetic, and chemo-preventive effects [35]. It has been clinically proven as a treatment for conditions such as diabetes, cardiovascular diseases, hypercholesterolemia, fatty liver, polycystic ovary syndrome, and cancer [34,35].

Berberine inhibits tumor growth, inducing apoptosis, and promoting cell cycle arrest in cancers such as leukemia, lung, and colorectal cancer and therefore it has a potential effect on anti-cancer activity [36,37]. Due to its poor absorption and stability, recently many of us started approaching nanotechnology-based, altering the structure at the C9 position, enhancing its bioavailability and therapeutic potential [38]. Notably, berberine is target-specific, stimulating apoptosis in tumor cells while sparing normal cells, making it a promising agent for cancer treatment [39].

Role of berberine in apoptosis via mitochondrial dysfunction and reactive oxygen species (ROS)-mediated pathways

Berberine plays an important role in inducing apoptosis in tumor cells by activating pro-apoptotic genes. Specifically, it alters the B-cell lymphoma-2 (Bcl-2) and Bcl-2-associated X protein (Bax), leading to a reduction in the mitochondrial membrane of tumor cells [40]. The disruption of the membrane stimulates the intrinsic apoptotic pathway and caspase cascade specifically (caspase-3 and caspase-8) resulting in the release of cytochrome C [41]. Furthermore, berberine has been shown to produce ROS in tumor cells, inducing apoptosis. ROS triggers the activation of the apoptosis signal-regulating kinase 1 (ASK1)/mitogen-activated protein kinase (MAPK)

signaling pathway [42]. ASK1, a serine/threonine protein kinase, participates in cell differentiation and apoptosis [43]. Once activated, ASK1 dissociates from thioredoxin-1 and induces cell death by activating the c-jun-NH2-kinase (JNK) and p38 MAPK pathways [44]. Targeting ROS generation is thus a promising strategy for the development of novel anti-cancer drugs.

In the previous research, it was demonstrated that berberine has a modulated effect on MAPK signaling pathways, including the extracellular signal-regulated kinase 1/2 (ERK1/2), p38 MAPK, and JNK pathways, to exhibit anti-cancer activity may be cell-type specific. It has been shown that berberine enhances the MAPK signaling pathway in human hepatoma (HepG2) and non-small cell lung cancer cells (A549) [45–47].

Therapeutic role of berberine *in vivo* models

In previous research, it was shown that the berberine exhibited a hepatoprotective effect which was observed in many *vivo* models (mice) and was compared with doxorubicin-induced liver toxicity. Pretreatment with berberine significantly reduces liver damage by improving hepatic function tests and minimizing histological changes such as hepatocyte necrosis and inflammatory infiltration cells [48]. The other research also conducted that the hepatotoxicity was induced by carbon tetrachloride and compared with berberine shown to reduce oxidative stress by maintaining superoxide dismutase and decreasing lipid peroxidation. Therefore, it would significantly alter the inflammatory response by reducing TNF- α , COX-2, and nitric oxide synthase which are mediators for inflammation. They observed that berberine decreased the level of transaminase and protected the hepatocellular membrane [49].

Tumor growth suppression in nude mice models

In an animal study, 4-week-old athymic male nude mice (BALB/c-nu/nu) were allowed to grow the tumor volume reached up to 5 mm \times 5 mm, and the mice were randomly divided into vehicle and berberine groups. The berberine was injected intraperitoneally with solvent [1% dimethyl sulfoxide (DMSO) and 99% phosphate-buffered saline (PBS)] and 25 mg/kg of berberine insolvent every day in NCI-H460 cells for the indicated duration, respectively. Once the tumor reached a volume up to 15 mm, the mice were sacrificed and xenografted. Remarkable changes in tumor growth and tumor weight of mice in the berberine-treated group were observed. Further, extensive necrosis was observed by histological staining in the treatment group but not seen in the vehicle group. The protein level of SIN3 Transcription Regulator Family Member A and DNA Topoisomerase 2-beta were downregulated in xenografts derived from berberine treated group which was consistent *in vitro* studies [50].

An *in vivo* study conducted on the oral administration of 8-cethylberberine (HBBR) at a dose of 10 mg/kg body weight could remarkably find tumor growth inhibited in xenograft mice in A549 cells. The rate of tumor growth suppression was 59.07% compared with the tumor control group [50]. It was found that 8-cethylberberine (HBBR) significantly

reduced tumor marker levels in the serum of A549 xenograft mice. It specifically decreased Neuron-specific by 37.7%, cytokeratin-19 (CYFRA 21-1) by 24.4%, and carbohydrate antigen 125 by 63.8% in the high-dose HBBR group (10 mg/kg) compared to the control group. Therefore, HBBR shows that it would effectively slow down the development process of tumors [51].

Pharmacokinetics and biodistribution of nanoparticles in *in vivo* models

The pharmacokinetics and biodistribution of nanoparticles are influenced by several factors such as size, surface charge, and composition which help to examine the organ accumulation, circulation time, and mechanism of their clearance. *In vivo*, studies have shown that the nanoparticles accumulate in the liver, spleen, and kidneys due to the mononuclear phagocyte system which has an impact on their therapeutic efficacy and potential toxicity. The pharmacokinetic profile was enhanced by the controlled drug release mechanisms including ester and amide hydrolysis by prolonging circulation and improving bioavailability. However, immunological barriers such as contamination of endotoxin and recognition of the immune system a significant challenges for clearing nanoparticles and systemic compatibility. Therefore, to overcome these challenges in optimizing nanomedicine, recently researchers started using conventional synergistic drug combinations by using nanotechnology in drug delivery. Due to a better understanding of the molecular mechanisms driving specific therapeutic combinations and the utilization of nanosized drug carriers, several nanoparticle formulations of synergistic drug combinations have advanced to clinical trials [52]. Recently, the main focus of nanomedicine research for the past years has been the invention of novel nanoparticle systems and the characterization of their physicochemical properties about their biological fate and functions. It is noted that the pharmacokinetics of medications encapsulated in nanoparticles differ from free pharmaceuticals in aqueous forms (longer half-life duration) [53].

Berberine copper oxide nano formulation by using *S. torvum* for drug delivery

Berberine, a key therapeutic agent in traditional Chinese and herbal medicine, is recognized for its potential in addressing various biological issues, including cancer. However, the permeability of the membrane is poor and it was categorized under the biopharmaceutical classification system as a class III drug [54]. Nanotechnology offers promising strategies to overcome this limitation by enhancing berberine's bioavailability and stability through nanoencapsulation approaches. These include magnetic nanoparticles, liposomes, chitosan nanoparticles, and pH-sensitive carriers, which improve targeted delivery and oral absorption [36]. Nanotechnology-based formulations could further enhance the efficacy and bioavailability of such natural compounds for cancer treatment [55].

The combination of berberine and CuONPs represents a promising strategy for the development of "Innovative cancer therapies" allowing for specific targets

and effective treatment. CuONPs not only act as carriers but also improve the drug delivery and stability of berberine. They have their inherent anti-cancer property due to their ability to induce oxidative stress in lung cancer cells. The dual-action approach, by combining the bioactivity of berberine with the CuONPs, offers a novel therapy for tackling lung cancer, which is a leading cause of global mortality. Moreover, the use of CuONPs in lung cancer therapy addresses key United Nations Sustainable Development Goals (UN SDGs) [56], our study highlights the integration of traditional medicine (*S. torvum*) with modern nanotechnology CuONPs supports for promoting innovative, sustainable, and effective treatment options while also minimizing environmental impact and recovery processes addressing unmet medical needs in tissue repairing and regenerative medicine (Goals 3 and 6). According to the UN SDGs, goal 12 (responsible consumption and production) and goal 13 (climate action) show up the potential by approaching “Green synthesis” by using *S. torvum* is a biogenic precursor which contributes to cancer therapy, wound healing and sustainable production methods and thereby reducing the environment impact on the usage of harmful chemicals.

Therefore, this study explores the combination of berberine Copper oxide nano formulation synthesized by using *S. torvum*, for lung cancer therapy addressing the research gap in their synergistic effects [57].

Therefore, the present study aims to focus on the synthesis of copper oxide nanoparticles mediated with *S. torvum* and berberine to enhance the therapeutic application in lung cancer cell lines.

MATERIALS AND METHODS

Berberine chloride form (Cat No: B3251-5G) and DMSO were procured from Sigma Aldrich. Copper sulphate, Trypsin (Gibco), Dulbecco’s Modified Eagle’s Medium (DMEM) (Gibco), and Fetal Bovine serum (Gibco) were supplied by LIFIC Pvt Ltd, Chennai. MTT Cell Proliferation Assay Kit (Cayman Chemical, 480 wells, Cat No: 0713865, Storage -4°C) was purchased from Synergy Scientific Services, Chennai. The glassware was cleansed and autoclaved

for the entire experimental work. The Tissue culture plates (96 wells, 6 wells, 12 wells) were used from the Tarson products limited and discarded properly.

Preparation of *S. torvum* extract

Fresh *S. torvum* fruit was obtained from a market in Chennai, India. The characterization and authentication of the plant material (*S. torvum*) were carried out at the Siddha Central Research Institute, Department of Pharmacognosy, Chennai, India (Authentication Number:1026.10122403). The fruit was thoroughly washed with distilled water and air-dried completely. The dried fruit was then finely ground into a powder using a mortar and pestle.

In the preparation of the extract, 1 g of the powdered fruit was added with 100 ml of distilled water. The solution was subjected to boiling for 15–20 minutes using a heating mantle set at a temperature of 70°C . The extraction was passed through Whatman no.1 filter paper to separate the solid particles. The filtered extract was consequently stored in a refrigerator for the future preparation of nanoformulation synthesis and it was represented in (Fig . 1).

Green synthesis of *S. torvum* mediated with copper oxide nanoparticles

To prepare the copper sulfate solution, 0.318 g of copper sulfate was dissolved in 70 ml of distilled water to achieve a 20 mM concentration. In the synthesis of CuONPs, 30 ml of *S. torvum* extract was added to 70 ml of the copper sulfate solution. The mixture was stirred at 750 rpm for 24 hours using a magnetic stirrer. UV-visible measurements were taken at 24–48-hour intervals to monitor the progress. This ratio allowed the bioactive compounds in the extract to function as both reducing and stabilizing agents in the formation of CuONPs. After the reaction, the nanoparticle pellet was collected by centrifuging at 8,000 rpm for 10 minutes. The resulting copper oxide nanoparticles underwent a purification process, during which the supernatant was discarded, and the pellet was washed twice using double-distilled water and ethanol. Finally, the pellet was stored in a

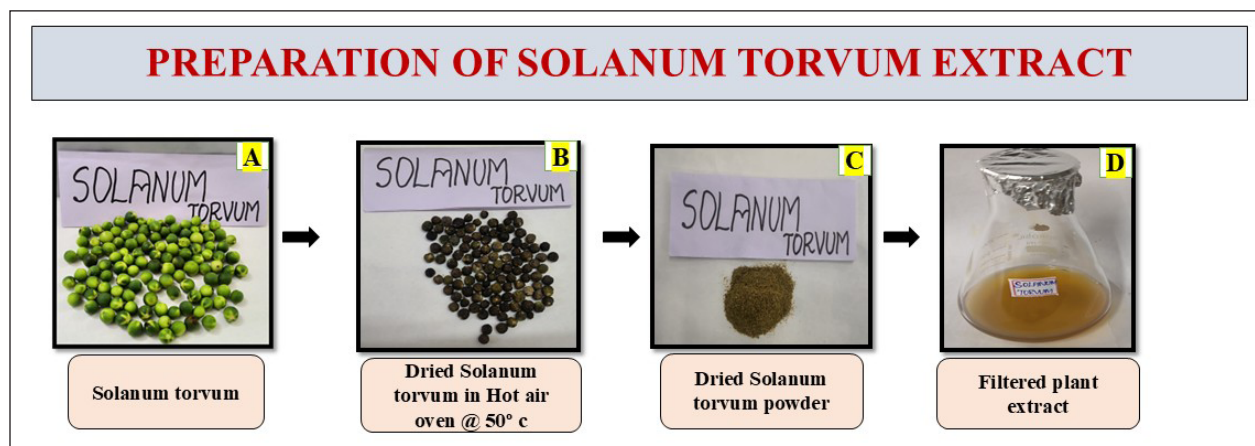


Figure 1. Represents the preparation of *S. torvum* extract.

sealed Eppendorf tube for further use in the preparation of the nano formulation (Fig. 2).

Synthesis of berberine copper oxide nano formulation using *S. torvum*

To prepare the berberine solution, 0.100 g (100 mg) of berberine was placed in a beaker.

1 ml of DMSO was used as a solvent to dissolve berberine to facilitate its incorporation into the synthesis process into the beaker, and gradually add 4 ml of PBS was used as a buffer solution, acting as a biocompatible medium to maintain physiological condition. Stir the mixture using a magnetic stirrer for 1 hour to ensure proper mixing of solution. 1 ml of the prepared berberine solution was added with 1 ml of the synthesized

Solanum torvum copper oxide nanoparticles. Combine them and subject the mixture to sonication for 30 minutes to achieve the nano formulation. In the process of sonication, perform a UV-visible spectroscopy analysis for preliminary confirmation of the nano formulation's synthesis. The combination of berberine and CuONPs may enhance the bioavailability when loaded as a berberine copper oxide nano formulation. To collect the pellet, place the petri dish in a hot air oven at 50°C and monitor it every 30 minutes. Once the pellet is completely dried, collect and store it in an Eppendorf centrifuge tube for further characterization and applications. The entire process was taken to complete for berberine copper oxide nanoparticles synthesis at 48 hours and only the berberine preparation took 6 hours at room temperature. The pH of the BBR-CuONPs suspension was found to be 7.48,

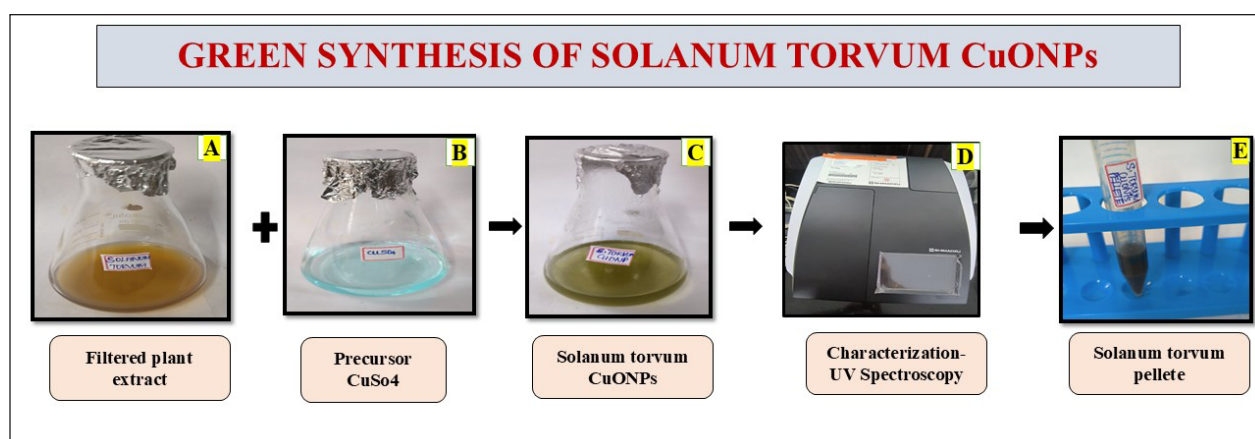


Figure 2. The diagram represents the green synthesis of the *S. torvum* mediated copper oxide nanoparticles.

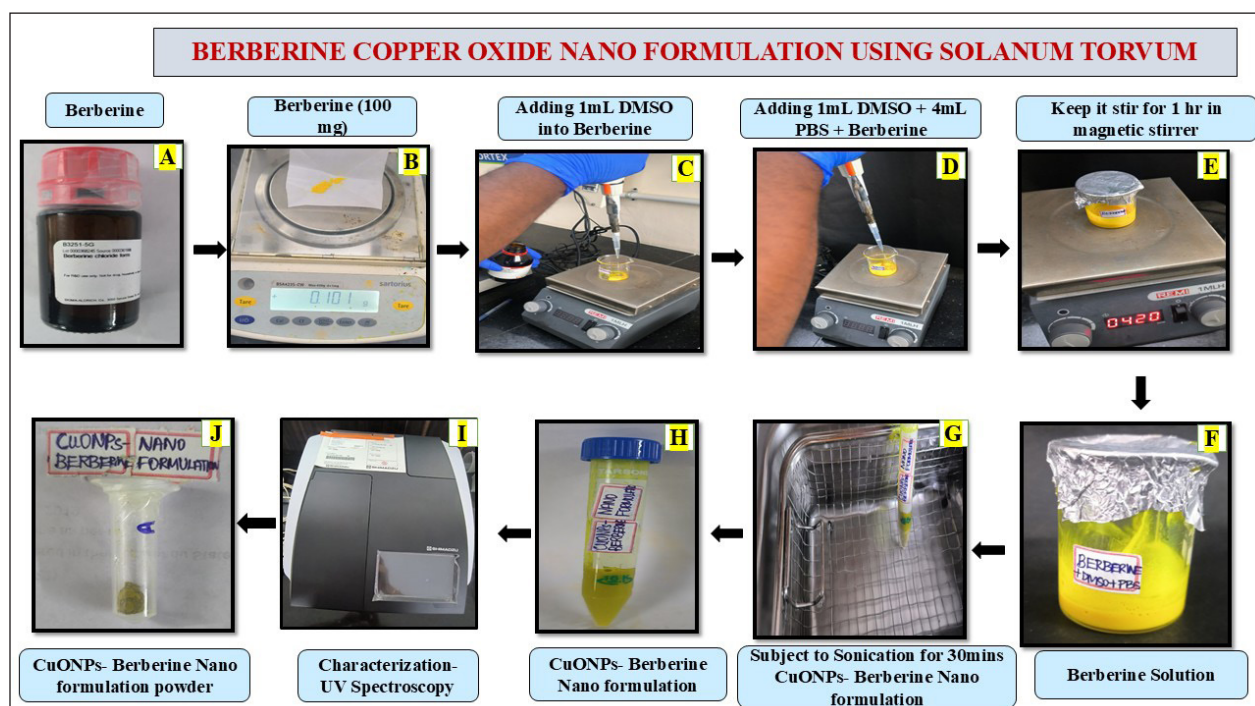


Figure 3. Pictorial representation for the preparation of berberine copper oxide nano formulation synthesized using *S. torvum*.

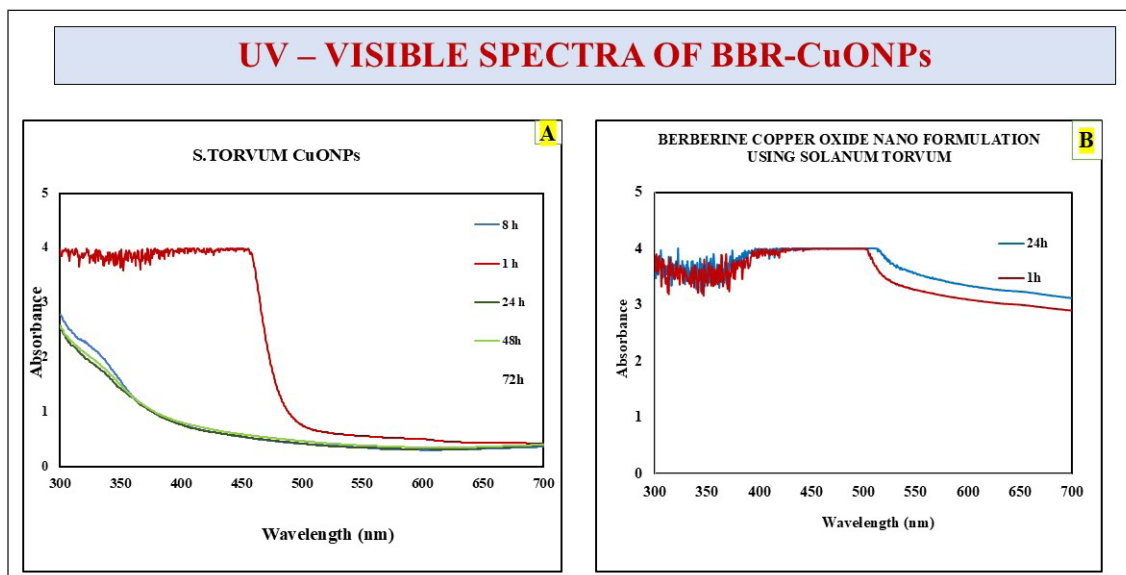


Figure 4. Depicts the UV-visible spectra of *S. torvum* CuONPs. A) *S. torvum* copper oxide nanoparticles, B) Berberine copper oxide nano formulation using *S. torvum*.

indicating a slightly alkaline nature. The yield of the berberine-loaded CuONPs was around 37 mg. The pictorial representation is shown in the (Fig. 3).

Characterization of berberine copper oxide nano formulation by using *S. torvum*

UV-visible spectrophotometer (UV-1900I) was used to measure the absorbance of the light at specific wavelengths and helps to quantify the concentration of a substance in a sample. The optical characteristics of copper oxide nanoparticles within the 200–700 nm wavelength. Fourier transform infrared (FT-IR) Spectroscopy (Perkin Elmer, Spectrum Two FTIR) was used to analyze the functional groups in the Berberine copper oxide nano formulation synthesized using *S. torvum*. Transmission electron microscopy (TEM) was used to analyze morphological features (TalosF200S High Resolution Scanning TEM). Additionally, an X-ray diffraction (XRD) (Unique D8 diffractometer) examination was performed to investigate the nanoparticles' phase structure and crystallinity.

Evaluating the anticancer activity of copper oxide nanoparticles mediated with berberine nano formulation

The MTT assay is a colorimetric method used to assess cell metabolic activity and is commonly employed in cell viability, proliferation, and cytotoxicity. The non-small lung cancer cell line (A549) was procured from the National Centre for Cell Science, Pune. A549 cells were cultured in DMEM supplemented with 10% heat-inactivated fetal bovine serum, 100 U/ml penicillin, and 100 mg/ml streptomycin. The cultures were maintained at 37°C in a humidified atmosphere with 5% CO₂. All experiments were triplicate, following good laboratory practices. When the cells reached 80% confluence, 1–1.5 ml of trypsin was added, and the cells were incubated for 5 minutes. The culture medium was then added, and the cells were gently mixed. The cell suspension was centrifuged at 3,500 rpm for

10 minutes to collect the cell pellet. Cell viability was assessed using the Trypan Blue exclusion method.

For the MTT assay, cells were seeded in a 96-well plate at a density of 5.0×10^3 cells per well in 200 μ l of culture medium and incubated in a CO₂ incubator for 24 hours. Once the cells adhered to the plate and reached 80% confluence, the medium was carefully discarded. The prepared *S. torvum* CuONPs-berberine nano formulation was added to the wells at concentrations of 10 μ g, 50 μ g, 100 μ g, and 200 μ g, and the cells were incubated for 24 hours.

After the drug treatment was over, the drug was removed, and 110 μ l of MTT reagent each well. The plates were incubated for 4 hours, followed by the addition of 100 μ l sodium dodecyl sulfate solution, and then incubated for an additional 4–18 hours and the plates were placed in a CO₂ incubator at 37°C. Absorbance was measured using a microplate reader at 570 nm. All assays were conducted in triplicate as described by Wu *et al.* [58]. The percentage of growth inhibition was calculated by using this formula described by [59] and the data obtained were used to generate a graph plotting cell viability percentage against extract concentrations. The optical density was analyzed using an ELISA reader (Biorad/imark, 21154) at 570 nm. The Graph Pad Prism (graph pad prism 10) software was used to analyze the data and to determine the IC₅₀ values.

$$\% \text{ Cell Viability} = (\text{Absorbance of treated cells} / \text{Absorbance of Control cells}) \times 100$$

$$\% \text{ Growth inhibition} = [(\text{Control OD} - \text{Sample OD}) / \text{Control OD}] \times 100$$

Wound healing assay

The wound healing assay is commonly used *in vitro* to investigate the coordinated migration and dynamics

of cell populations using scratch assay. The migration assay was assessed using berberine copper oxide nano formulation synthesized with *S. torvum*. The non-small cell lung cancer (A549) cells (5×10^5) were seeded in a 6-well plate and incubated for 24–48 hours. The monolayer of 80% confluent was scratched with a yellow tip to create a migrating zone, followed by washing with PBS to remove debris. The drug was then added at concentrations of 0, 10, 50, 100, and 200 $\mu\text{g/ml}$, and the plates were incubated in a CO_2 incubator. The distance of the migrating zone was photographed in 0, 24 hours, and 48 hours using an Inverted Fluorescent microscope (Accu-Scope-EXI-310-FL3) under a high-power magnification [60]. Then, the plates were washed with PBS to remove any remaining drug, followed by the methanol and acetone fixation method. Finally, a few drops of crystal violet were added, and the plates were stained for 15 minutes before observing the images under an inverted microscope (Accuscope- EXI- 310-FL3) and the software (Captavision 2.0) was provided by the company for capturing the cell migration images. The quantitative examination of cell migration was conducted using an average wound space from random fields of view. The following formula was used to determine the percentage change in the wound space [61].

% Change in Wound Space =	$\frac{(\text{Average Space at Time 0 h}) - (\text{Average Space at Time 48h}) \times 100}{(\text{Average Space at Time 0h})}$
Relative cell migration =	$\frac{\% \text{Change in Wound Space (Control Cells)}}{\% \text{Change in Wound Space (Treated Cells)}}$

STATISTICAL ANALYSIS

The experiments were replicated three times ($n = 3$) and the outcomes were expressed as Mean \pm Standard Deviation (Mean \pm S.D). IBM SPSS Statistics version 19 (IBM, Chicago, USA) was used to evaluate all the statistical analyses. The Shapiro-Wilk test was employed to assess data normality, and since the data exhibited a normal distribution, parametric tests were utilized. Intra-group comparisons were conducted using the paired *t*-test, while inter-group differences were evaluated through One-Way ANOVA. Different concentrations of the standard drugs and the test samples were evaluated using a $p \leq 0.05$ significance threshold.

RESULTS AND DISCUSSION

UV-Vis absorption spectroscopy of copper oxide nanoparticles and nano formulations

UV-visible spectroscopy is a technique widely used for the determination of the concentration, size, and optical properties of the sample. It provides valuable insights into their absorption peaks, revealing the molecular structure and nanoscale behavior. For CuONPs, the absorption in the range of 400–450 nm corresponds to electronic transitions characteristic of these nanoparticles so it was improved with earlier research [62]. The sharp decline observed in the absorbance around 400–

500 nm is typical of smaller or less-structured copper oxide nanoparticles. The gradual decrease in absorbance over time indicates changes in nanoparticle behavior, such as aggregation or reduced colloidal stability. The final confirmation for the synthesis of the copper oxide nanoparticles was observed that initially, it was a golden yellow color (Fig. 1D) transformed into an olive-green color (Fig. 1F) which signifies the completion of synthesis has shown in Figure 4A.

In the case of the CuONPs mediated with berberine nano formulation, a consistent and broad absorbance is observed within the 350–450 nm range (Fig. 10), and it was highlighted in earlier research evident that berberine has the highest absorbance at 422 nm [63]. The increased absorbance intensity in the berberine nano formulation reflects enhanced optical properties, likely due to interactions between CuONPs and berberine. These interactions will improve light absorption and nanoparticle stability. Additionally, a slight redshift in the absorption peak suggests stronger bonding or conjugation between CuONPs and berberine molecules. Overall, the incorporation of berberine enhances the optical stability and absorption characteristics of the nanoparticles, potentially improving their functional properties for applications such as drug delivery.

Transmission electron microscope

The TEM was employed to study the morphology, size, shape, surface properties, and chemical composition of the nano formulation at the nanoscale. It provided detailed visualization of the nanoparticle structure and interactions, which is critical for optimizing their performance in various applications, including drug delivery, particularly in their interactions with biological cells. TEM images were analyzed using ImageJ software, which enabled the determination of the average size of the copper nanoparticles in the berberine-mediated nano formulation. The nanoparticles were found to

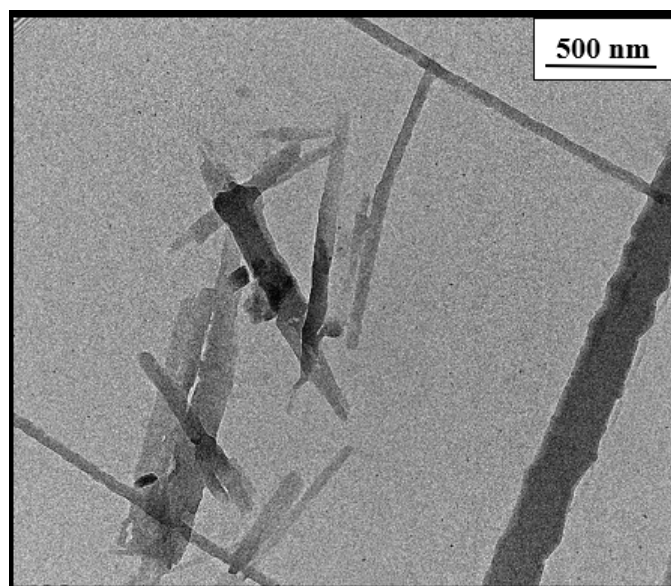


Figure 5. TEM: berberine copper oxide berberine nano formulation using *S. torvum*.

have an average diameter of approximately 10–50 nm and lengths ranging from 100 nm to several 100 nanometers. The lower and higher magnification of TEM images ranges from 36,000X to lattice fringes to 10,50,000X. The size distribution of the berberine copper oxide nano formulation is shown in (Fig. 5). The observed shape of the nanoparticles was nanorods. The TEM images have been authenticated following rigorous validation protocols. The instrument settings, sample preparation procedures, and calibration techniques have been meticulously documented to ensure accuracy (Talos F200S High-Resolution Scanning TEM). Previous research has also shown that many copper nanoparticles with a size of about 35 nm are uniformly distributed [64].

Fourier transform infrared spectroscopy

FTIR is an analytical tool used for the identification of chemical composition, molecular structure, and functional group of the sample. The chemical composition of the samples was analyzed by Attenuated Total Reflectance–FTIR (PerkinElmer Spectrum Two FTIR) in the spectral region of 4,000–400 cm^{-1} wavelength with 4 cm^{-1} resolutions at total scan of 64 scans per sample.

The analysis of FTIR for CUONPs mediated with *S. torvum* and berberine nano formulation showed significant variations in the chemical composition, highlighting the bioactive functional groups present in the formulation (Table 1). The peaks of berberine chloride at 3,547.7 cm^{-1} and 3,298.2 cm^{-1} (35) associated with O–H stretch (hydroxyl group), indicate the presence of alcohols or phenolic compounds known for their antioxidant properties, hydrogen bonding, and reactivity. These hydroxyl vibrations likely result from interactions between *S. torvum* extracts and berberine during nanoparticle synthesis which is significant for drug formulation and wound healing due to its water solubility and reactivity. A peak at 2,918.7 cm^{-1} , which corresponds to C–H stretch (methyl group), is significant for the involvement of alkyl chains, possibly from lipid-like compounds present in *S. torvum*. The aromatic ring vibration at 1,504.7 cm^{-1} , associated with C=C stretch (bending vibration in phenolic structure, [65], further emphasizes the bioactivity of the nanoformulation which plays an important role in electron delocalization, which can stabilize free radicals and make its phenolic more effective and neutralize the oxidative

stress. This aromatic structure contributes to the formulation's binding affinity with biological targets, potentially improving its therapeutic efficacy and modulating cellular signaling pathways. The C–O–C bonding was observed at 1,032.4 cm^{-1} [65] peak which indicates the presence of glycosidic linkages or ester groups, potentially enhancing nanoparticle stability. The functional group C–H bending at 828.8 cm^{-1} signifies aromatic systems, the C–S stretch at 615.74 cm^{-1} (chloride as halide band [65] which was strongly evident in the previous research the frequency ranges of FTIR analysis are mostly similar to our test results compare with the reference articles (Fig. 6). The C–S bonding indicates the presence of sulfur-containing compounds is likely to produce the secondary metabolites in plants during stress potentially for the plant's defense mechanism.

Finally, the formulated berberine compound strongly suggests the presence of antioxidant and regenerative properties which could promote cellular healing, the anti-inflammatory and anticancer properties of berberine, in synergy with CUONPs, could induce apoptosis and inhibit tumor

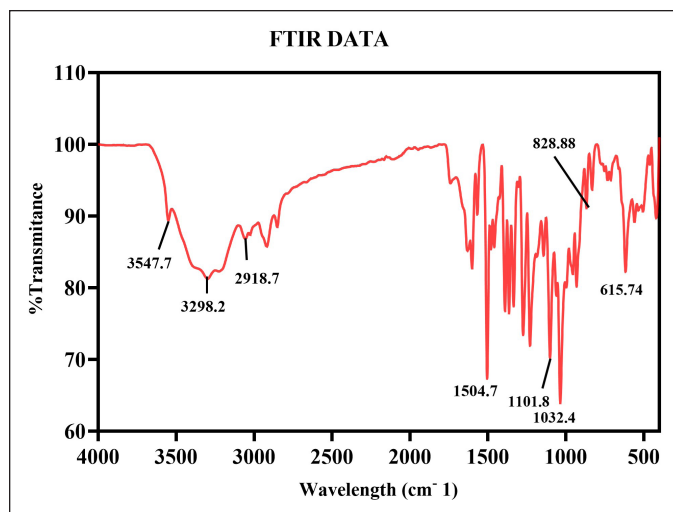


Figure 6. FT-IR spectroscopy of berberine copper oxide nano formulation using *S. torvum*.

Table 1. FTIR Spectra of *S. torvum* mediated with berberine copper oxide formulation.

Wavelength (cm^{-1}) (Berberine copper oxide nano formulation)	Wavelength (cm^{-1}) (Reference article)	Functional moiety
3,547.7	3,550–3,450	Hydroxyl compound
3,298.2	3,400–3,200	Hydroxyl compound
2,918.7	2,854–2,926	Methyl group
1,504.7	1,458–1,591	Phenol ring
1,032.4	1,150–911	C–O–C group
828.8	858–733	C–H group
615.74	600–700	C–S linkage

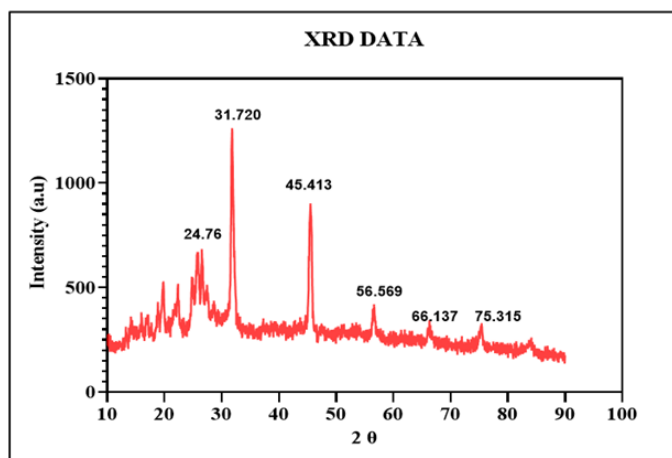


Figure 7. XRD analysis of synthesized BBR-CuONPs nanoparticles.

growth. However, the nanoformulations show that interact with biological systems at the molecular level suggesting it is a dual-action mechanism for tissue regeneration and anticancer activity. Further investigation is needed to examine its biological efficacy, stability, and biocompatibility, ensuring safe and effective application in anticancer and wound healing therapies.

XRD analysis

The XRD analysis is a technique that provides detailed information about the crystalline structure, size, and physical properties of the materials. The XRD patterns of the berberine-loaded CUONPs functionalized reveal the formation of CuO nanoparticles with the diffraction's peaks at 24.76°, 31.720°, 45.413°, 56.569°, 66.137°, and 75.315° (2θ values) related to (002), (110), (112), (020), (022), and (222). These peaks correspond to specific crystal planes of copper oxide, confirming the successful synthesis of crystalline CuO nanoparticles. The major peaks at 31.720° and 45.413° are characteristic of monoclinic copper (II) CuO, and the XRD pattern matches with JCPDS card no. 01-080-1916 (Fig. 7). The average crystallite size of CuO nanoparticles was determined using the Debye–Scherrer equation. In this formula, D represents the average nanoparticle diameter, K is the Scherrer constant, λ denotes the x-ray diffraction wavelength (015.406 nm), β is the full width at half maximum, and θ refers to the Bragg angle (in degrees) [66]. Based on this calculation, the estimated crystallite size of the synthesized CuO nanoparticles falls within the range of 20.35 nm. Therefore, the presence of a crystalline CuO phase indicates good crystallinity, essential for the stability, and bioactivity of the nanoparticles [67]. The overall XRD pattern indicates well-formed crystalline copper oxide, with potential modifications due to the incorporation of *S. torvum* and berberine, which may influence the crystal structure or introduce new phases. This suggests that the functionalization process enhances the nanoparticle's bioactivity, making them suitable for various

therapeutic applications, including anticancer and wound healing.

$$D = K\lambda / \beta \cos\theta$$

Anti-cancer activity of berberine copper oxide nanoformulation by using *S. torvum*

Based on the previous reports, the biosynthesized CuONPs mediated with *S. torvum* have excellent cytotoxicity effects against human lung cancer cells and were analyzed using MTT assay followed by the recent report [68]. Previous research works have reported the inhibitory effect of berberine on cell proliferation, and metastasis in various cancers such as colorectal, prostate, lung, ovarian, and glioma cancers [37,69,70]. It regulates the cell cycle by inducing cell cycle arrest at the G1 phase in tumor cells. While used at lower concentrations, berberine inhibits tumor cell growth at the G1 phase, whereas higher concentrations cause growth arrest at the G2/M phase of the cell cycle [71]. The anti-cancer activity of berberine has been linked to the downregulation of adenosine monophosphate-activated protein kinase and hypoxia-inducible factor 1-alpha, inhibition of cell proliferation, inducing apoptosis, angiogenesis arrest, and suppression of tumor growths [72].

Comparative cytotoxicity of berberine-loaded CuONPs on A549 cells

The result of the MTT analysis for the CuONPs mediated with *S. torvum* berberine formulation interprets dose-dependent inhibition of cell viability with increasing concentrations of the test sample. The bar graph represents the A549 cell viability assay evaluating the cytotoxic effects of the BBR-CuONPs and comparisons were made with the chemotherapeutic drug cisplatin at the different drug concentrations (10, 50, 100, and 200 µg/ml). The percentage of cell viability is plotted on the y-axis, while different treatment groups are on the x-axis. The percentage for the viability of

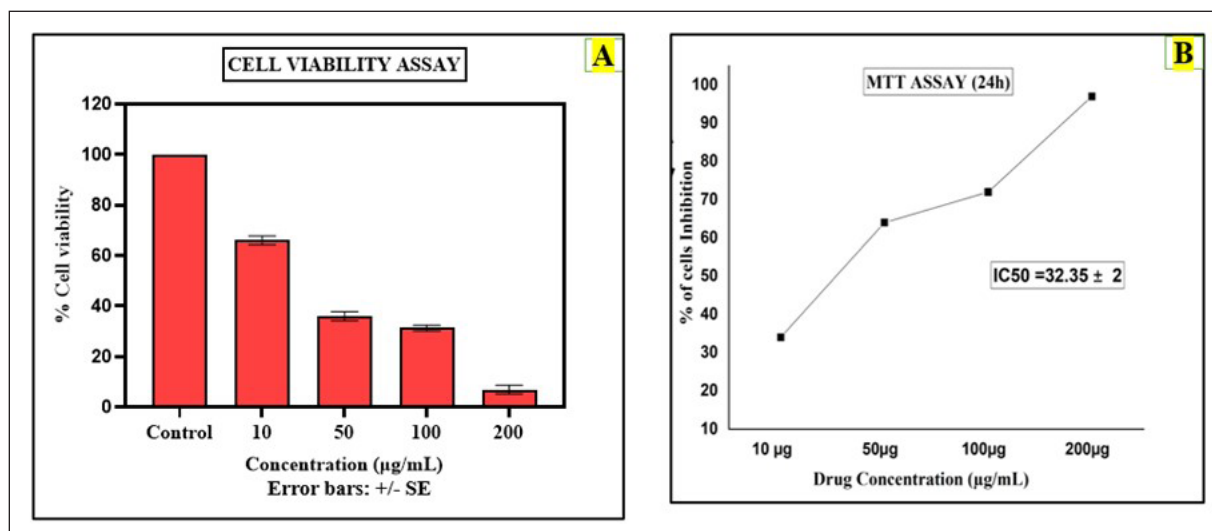


Figure 8. Anti-cancer activity (MTT assay): A) The bar diagram shows the assessment of cell viability for berberine copper oxide nanoparticles B) The graphical representation shows the cytotoxicity effect of berberine copper oxide nanoparticles in A549 cell lines.

the cells is decreased by 100%, 68%, 38%, 30%, and 5% when the cells are exposed to the drug concentration of control, 10, 50, 100, and 200 $\mu\text{g/ml}$, respectively. In the MTT assay, the anti-cancer activity for the drug concentration of 10 $\mu\text{g/ml}$, the inhibition percentage is 32.16%, showing that it has mild cytotoxic activity. As the concentration increases to 50 $\mu\text{g/ml}$, the percentage of inhibition rises significantly to 62.37%, indicating moderate effectiveness. At 100 $\mu\text{g/ml}$, the inhibition reaches 69.69%, suggesting that it is strongly effective at this concentration as shown in (Fig. 8B). Finally, at 200 $\mu\text{g/ml}$, the inhibition is almost maximum at 94.85%, the capacity of the berberine nano formulation [73] suggesting that the combination of BBR-CuONPs strongly synergizes, leading to severe toxicity in A549 cells.

The cell viability of the copper oxide nanoparticles in A549 cells was observed at the dose of 10 $\mu\text{g/ml}$ was around 79% and as the concentration increased to 50, 100 200 $\mu\text{g/ml}$ gradually, the cell viability decreased to 41%, 38%, and 29%, respectively. For the free berberine, the viability of cells at 10 $\mu\text{g/ml}$ (72%) is slightly lower than CuONPs, and the sharp decline was observed at the concentrations of 50 (39%) and 100 $\mu\text{g/ml}$ (33%), and 200 $\mu\text{g/ml}$ (17%). When compared to free berberine with copper oxide nanoparticles, CuONPs showed higher cell viability in A549 cells. Therefore, CuONPs and Berberine (BBR) exhibit dose-dependent toxicity, with more significant reductions in cell viability at higher concentrations. BBR-CuONPs show strong synergistic toxicity, leading to the lowest cell viability at higher concentrations, indicating that the combination treatment is more effective than the individual components at reducing cell survival (Fig. 9A).

In the cytotoxicity analysis, DMSO was used as a solvent control, as berberine was dissolved in DMSO for the experiment. DMSO is commonly employed in cell-based assays, and as a solvent-only control, it helps determine if any observed cytotoxic effects are due to the test compounds rather than the solvent itself. The cell viability observed in the DMSO group was around 98.9%, very close to the control group (E), showing 100% viability. This indicates that the DMSO does not induce cytotoxicity in A549 lung cancer cells. Thus, any effects observed in the treatment groups can be confidently attributed to the compounds being tested rather than the solvent.

In previous research, Caco-2/TC7 colon tumor cells were treated with DMSO with concentrations of up to 10% in the colon tumor cells. The results showed that DMSO did not significantly affect the cell viability, permeability, or tight junctions (connections between cells). The lactate dehydrogenase release is a marker for cell damage and neutral red was used to measure cell viability but did not show significant changes, suggesting that 10% DMSO is non-toxic to these cells. Therefore, the DMSO-treated cells do not cause significant cytotoxicity or affect cell function, making it a suitable solvent for experiments without interfering with the results [74].

One-way ANOVA proved statistically significant differences in cell viability of A549 cells between the different drug formulations and concentrations used in the study (p -value < 0.05). The mean cell viability of the combination drug BBR-CuONPs against A549 cells was significantly lesser than

CuONPs drug formulation and BBR drug formulation at all the concentrations used in the study (p -value < 0.05). However, it was also noted that the cell viability of A549 cells was lesser in cisplatin (positive control) than in all other drug formulations, thus proving its gold-standard effect on cancer cells.

The cytotoxicity effect of free berberine and copper oxide nanoparticles was calculated by using IC_{50} values 24.92 ± 2 $\mu\text{g/ml}$ and 23.31 ± 2 $\mu\text{g/ml}$, respectively, the inhibitory effect was almost similar for these two drugs in A549 cells. There was an increase in the cell inhibition of all the groups with an increase in the concentration. Though, the IC_{50} value of 32.35 ± 2 $\mu\text{g/ml}$, the cytotoxic effect for BBR- CuONPs by using nanoformulation method helps to control the release effect, where berberine is gradually released from the CuONPs, reducing its immediate cytotoxicity while potentially enhancing long-term effects and selectively targeted cancer cells. In the gold standard chemotherapeutic drug such as cisplatin, the cytotoxicity is high when compared to BBR-CuONPs but still cisplatin has an impact on both cancer and normal cells and produces toxicities in humans. The IC_{50} value was calculated by using software (graph pad Prism 10) indicating the concentration required to inhibit 50% of cell viability. The dose-response

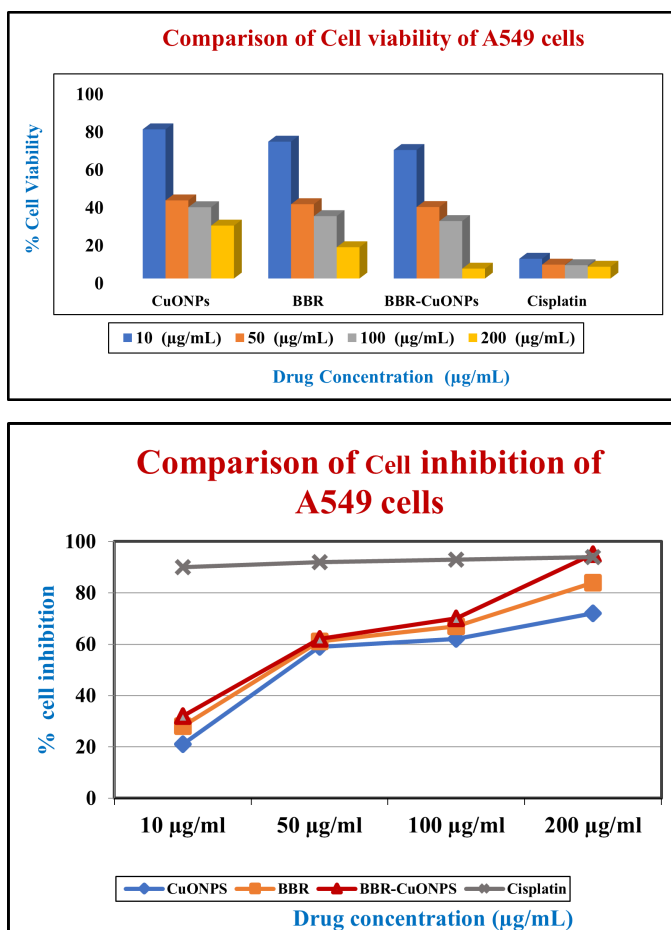


Figure 9. The pictorial representation of the anti-cancer activity in A549 cells A) The bar diagram compares cell viability for CuONPs, BBR, and BBR-CuONPs of A549 cells. B) The graphical representation depicted the comparison of cell inhibition for CuONPs, BBR, and BBR-CuONPs of A549 cells.

Table 2. Mean IC₅₀ values of BBR, CuONPS, BBR- CuONPs.

Drug	N	Mean ± Std deviation (95 % CI)
Berberine	3	24.92 ± 0.42 (23.86–25.97) *
CuONPS	3	23.37 ± 0.40 (22.36–24.37) *
Berberine-CuONPS	3	32.35 ± 0.35 (31.48–33.21) *

*95% confidence interval for mean.

curve follows a sigmoidal trend, with a plateau observed at higher concentrations (beyond 200 µg), where further increases in concentration do not significantly enhance the inhibitory effect. Overall, the effective cytotoxic activity with substantial inhibition was observed at concentrations within 50 µg/ml. The synergistic effect between Berberine and CuONPs makes the combination more potent than individual treatments and may contribute to sustained anti-cancer activity over a long time rather than immediate cell death (Fig. 9B).

One-way ANOVA proved statistically significant differences in cell inhibition of A549 cells between the different drug formulations and concentrations used in the study (p -value < 0.001). The combination drug BBR-CuONPs had higher cell inhibition on A549 cells than CuONPs drug formulation and BBR drug formulation at all the concentrations used in the study and these differences were found to be statistically significant (p -value < 0.05). However, Cisplatin produced the highest cell inhibition towards A549 cells indicating its gold-standard effect on cancer cells. Table 2 shows the Mean IC₅₀ values of berberine, copper oxide nanoparticles, and BBR-CuONPs.

The research has shown that copper nanoparticles exhibited cytotoxic and genotoxic effects on human skin epidermal cells, due to mitochondrial pathways triggered by reactive oxygen species [75]. But copper nanoparticles with different concentrations (10, 20, 50, 100, and 200 µg/ml) observed very minimal toxicity to the cells which promoted cell proliferation may be due to the size of copper nanoparticles where the unabsorbed ones are removed by the colon [76]. In cell viability assay has shown a remarkable dose-dependent manner, i.e., the highest concentration promotes more proliferation of the cells. Copper involves the skin regeneration and angiogenesis observed from the animal model by accelerating the healing process through VEGF and angiogenesis by inducing hypoxia-induced factor-1-alpha (HIF-1α) action whereas copper enhances HIF-1α expression. HIF-1α plays an important role in critical wound healing and motifs the promoter and putative enhancer regions of HIF-1-regulated genes [77].

Comparative cytotoxicity of berberine-loaded CuONPs and cisplatin on normal cells human embryonic kidney (HEK)

The HEK cell viability assay evaluates the cytotoxic effects of CuONPs, BBR, Berberine-Loaded CuONPs (BBR-CuONPs), and Cisplatin on normal HEK cells at different concentrations (10, 50, 100, and 200 µg/ml). The cell viability for copper oxide nanoparticles shows that (~100%) at lower concentrations (10 and 50 µg/ml), and moderate reduction was observed at 99% and 75% in higher concentrations 100 and 200 µg/ml, respectively. Therefore, it suggests minimal toxicity to normal cells in higher concentrations (200 µg/ml). For the

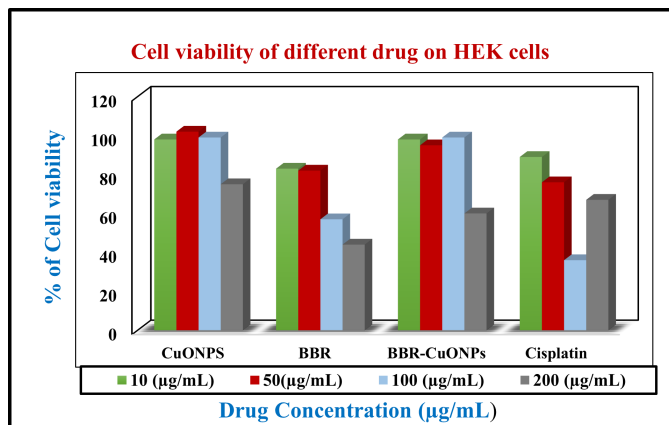


Figure 10. The bar diagram represents the cell viability for CuONPs, BBR, and BBR-CuONPs in HEK cells.

berberine, the viability of the cells was observed at almost 85% for both 10 µg/ml and 50 µg/ml, and 57% and 44% at the concentrations of 100 and 200 µg/ml indicating mild toxicity in normal cells compared with CuONPs. In the case berberine loaded CuONPs, the viability of cells shows the highest percentages of 98%, 95%, 99%, and 60% at the concentrations of 10, 50, 100, and 200 µg/ml indicating biocompatibility and viability drops but remains higher compared to cancer cells. In the cisplatin treatment, viability percentages 89%, 76%, 36%, and 67% for the same concentration, there is a significant reduction in HEK cell viability at higher concentrations (100 and 200 µg/ml) indicating high toxicity to normal cells, consistent with known side effects of chemotherapy (Fig. 11). In previous research, Cisplatin-induced injury in renal vasculature and resulted in decreased blood flow and ischemic injury of the kidneys, contributing to a decline in the glomerular filtration rate. These events, together, culminate in the loss of renal function during cisplatin nephrotoxicity, triggering acute renal failure [78].

In HEK normal cells, the cytotoxic effect for the CuONPs shows a relatively low inhibition at lower concentrations (10 µg/ml), but a significant increase at higher doses (100 and 200 µg/ml). Berberine also displays higher inhibition than compared to CuONPs, especially at higher concentrations. BBR-CuONPs show a marked increase in inhibition at 200 µg/ml around 40%, and indicate selective toxicity against A549 cells. Cisplatin has an inhibitory effect in both cancer and normal cells and high toxicity to normal cells.

The previous study was conducted on copper-containing complexes that have potential applications in cancer cells, exhibiting that copper complexes that are believed to be less toxic than cisplatin have a different mechanism of action. Compared to other metals, the geometry of copper-containing complexes facilitates their interaction with the DNA helix. Copper-containing complexes have been shown to have anti-cancer activity [79].

In a mice model study, berberine-loaded silver nanoparticles were treated with breast cancer (MCF-7) cells it was found that the tumor volume and weight were reduced

by inhibiting MCF-7 cell proliferation without reducing the body weight of the mice model. It was observed that there were efficient entries and changes made in the breast cancer cell releases of the cytoplasm. The berberine and nanoparticles inducing cytotoxic effects and triggering the apoptosis interfere with HIF-1 alpha and inhibition of PI3K/AKT and Ras/Raf/ERK proteins expression in signaling pathways and generating ROS, respectively [80].

In previous research, it has been proven that berberine was combined with silver nanoparticles along with folic acid and polyethylene glycol (FA-PEG@BBR-AgNPs) for breast cancer treatment by overcoming toxic effects caused by chemotherapeutic drugs [80]. Taebpour *et al.* [81] also investigated the cytotoxicity effect of berberine encapsulated in Poly (lactic-co-glycolic) acid (PLGA) nanoparticles compared with free BBR in MCF-7 breast cancer cells. The IC_{50} value for the berberine nanoparticles was found to be lower (42.39 $\mu\text{g/ml}$) compared with that of free berberine (80.18 $\mu\text{g/ml}$), significantly showing its anticancer activity. The researcher observed that PLGA-BBR was found to have no cytotoxicity in normal human cells (HFF and MCF-10A), suggesting its potential for selective cancer therapy with minimal off-target effects. Nano formulations derived from natural products such as berberine have shown anticancer activity against various lung cancers [82]. Therefore, combining berberine-loaded CuONPs helps in suppressing A549 cells found to cause Reactive oxygen species-mediated cytotoxicity and stimulate pro-inflammatory response which could remarkably improve the efficacy of cancer treatments and better therapeutic outcomes [83].

Wound healing assay

The effects of berberine copper oxide nanoparticles were evaluated by using a wound-healing assay. It was observed that the berberine nano formulation, the dose-dependent suppressed the wound healing in A549 cell lines induced at the different concentrations and different time intervals at 0, 24, and 48 hours post-injury. The control group exhibited the highest percentage of cell movement in the

wound healing space, indicating significant cell migration was noted in the absence of the drug. In contrast, the different drug concentrations (10, 50, 100, and 200 $\mu\text{g/ml}$) were treated with the A549 cells, the result has shown as the dosage increased there was a progressive reduction in wound space closure, with the highest inhibition was observed at 100 $\mu\text{g/ml}$ and 200 $\mu\text{g/ml}$ with minimal wound closure, demonstrating strong inhibition of migration in 24–48 hours than compare with the other groups (10 $\mu\text{g/ml}$ and 50 $\mu\text{g/ml}$) it was partially wound closure at 48 hours, indicating some inhibition. At the concentration of 200 $\mu\text{g/ml}$, almost complete inhibition of the cell migration is observed in 24–48 hours, with a persistent wound gap and suggesting strong anti-metastatic potential. Therefore, drug dosage-dependent concentration potentially suppresses the cell migration and targets the cancer cells by enhancing the cytotoxicity effects. BBR-CuONPs exhibit strong anti-migratory and possibly cytotoxic effects on cancer cells. These copper oxide nanoparticles could serve as potential anti-metastatic agents by inhibiting cell migration and matrix metalloproteinase (MMP) activity. However, the crystal violet staining, shows that in the control group, the cell becomes dense confirming high cell viability and proliferation. In the treatment group, as the drug concentration increases, the stained cell density decreases indicating reduced cell migration and possible cytotoxic effects leading to lower cell survival (Fig. 12). This indicates that the nanoformulation effectively suppresses cell migration, a critical process in tumor metastasis at lower concentrations. These findings highlight the anti-migratory potential of the formulation, reinforcing its promise as a therapeutic agent for migrating cancer metastasis.

The bar diagram represents the percentage changes in wound space of berberine-loaded CuONPs was calculated by using the formula $[\% \text{Change in Wound Space} = (\text{Average Space at Time 0 hour}) - (\text{Average Space at Time 48 hours}) / (\text{Average Space at Time 0 hours}) \times 100]$. It was observed that the drug concentration at 10, 50, 100, and 200 $\mu\text{g/ml}$ and the percentage changes in wound space were 15.99%, 9.93%, 9.34%, and 6.14%, respectively, in 48 hours. The highest

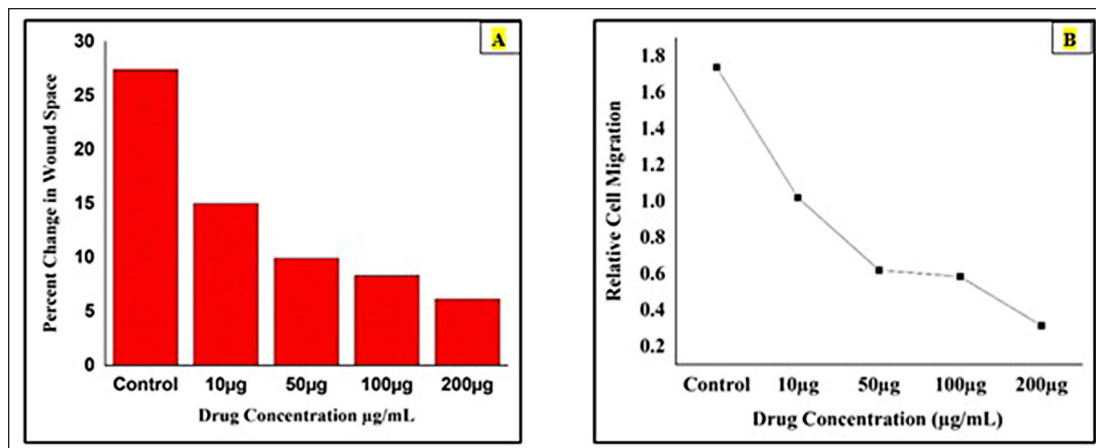


Figure 11. The pictorial diagram shows the cell migration analysis. A) The bar diagram shows the percentage gap in wound space. B) The graph illustrates the relative cell migration on A549 cells.

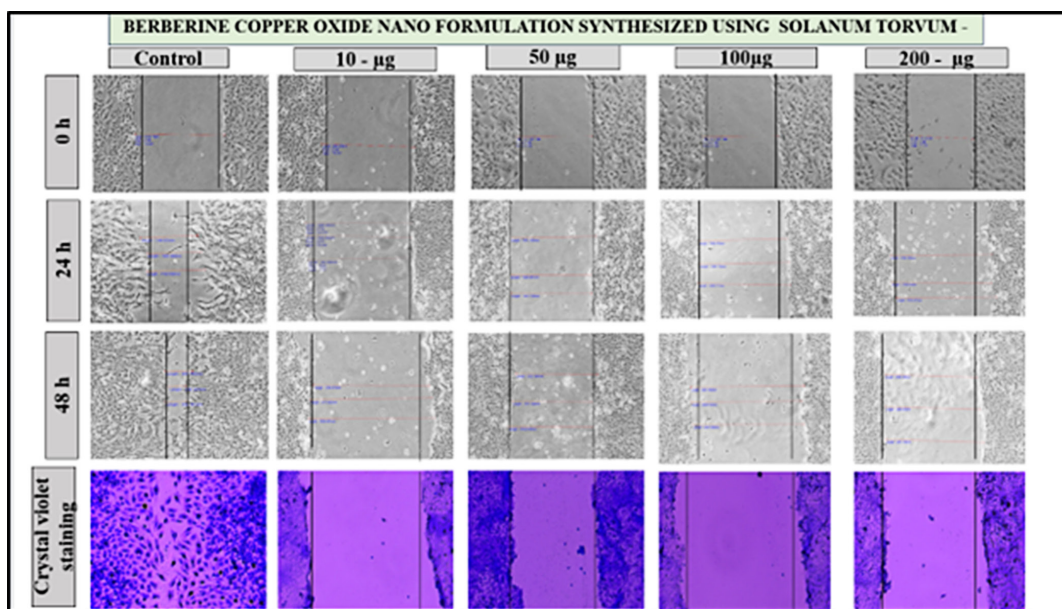


Figure 12. The pictorial diagram shows the cell migration for the drug concentration of control, 10, 50, 100, and 200 µg/ml at 0, 24, 48 hours for the berberine copper oxide nano formulation using *S. torvum*.

Table 3. Intergroup and Intra-group comparisons of distance of cell migration between the study groups.

	0 hours (T ₁)	24 hours (T ₂)	48 hours (T ₃)	<i>p</i> -value ^a	<i>p</i> -value ^b	<i>p</i> -value ^c
Control	1646 ± 55.01	1382.67 ± 50.83	418.33 ± 33.62	0.03*	0.002*	<0.001**
10 µg	2230.67 ± 227.45	1574.67 ± 70.51	1086.33 ± 108.85	0.04*	0.02*	0.002*
50 µg	1997.33 ± 106.43	1874.67 ± 110.21	1946.0 ± 156.64	0.006*	0.71	0.60
100 µg	2241.33 ± 225.76	2032 ± 65.96	1923.67 ± 360.85	0.24	0.10	0.61
200 µg	2266.67 ± 249.10	2041.67 ± 184.91	2079.67 ± 83.76	0.31	0.21	0.71
<i>p</i> -value ^d	<0.001**	<0.001**	<0.001**			

***p*-value < 0.001 – highly statistically significant

^{a, b, c} Paired *t*-test (intra group comparisons); ^a0 hours vs 24 hours; ^b0 hours versus 48 hours; ^c24 hours versus 48 hours ^dOne Way ANOVA (inter group comparisons); **p*-value < 0.05-statistically significant.

percentage, of changes in wound space was observed in the control group 29.42% in the absence of drugs. Therefore, the higher drug concentration (50–200 µg/ml) group significantly reduced wound closure, possibly due to cytotoxic effects. At the concentration of 200 µg/ml, had the least migration, suggesting strong inhibitory. (Fig. 11A).

The graph representing the relative cell migration of berberine copper oxide nanoparticles was calculated by using this formula Relative cell migration = %Change in wound space (Treated cells) / %Change in wound space (Control). The cells were treated with the different concentrations at 10, 50, 100, and 200 µg/ml and the values were obtained as 1.838, 2.953, 3.149, and 4.79, respectively. Therefore, the highest concentration 200 µg/ml (4.79) indicates the strongest inhibition and significantly reduces the cell migration possibly due to cytotoxic effects compared with the control group (1.0). When these values are plotted on the graph, the relative cell migration for the

above-mentioned concentration values are 1.0, 0.62, 0.548, and 0.348 were obtained. Hence, the relative cell migration range was inversely proportional to the dose concentration (Fig. 11 B).

Table 3 shows the evidence for the inter and intra-group comparison for 0, 24, and 48 hours and its statistically significant *p*-value < 0.05. This table shows intergroup and intra-group comparisons of migration distance. There was a significant decrease in migration distance at all three-time intervals (T1-T2, T1-T3, T2-T3) in the control group (*p*-value < 0.05, respectively). Similarly, there was a significant decrease in migration distance at all three-time intervals (T1-T2, T1-T3, T2-T3) in nanoformulation of 10 µg/ml of BBR-CuONPS. Nano formulation of 50 µg/ml of BBR-CuONPs showed a significant reduction in migration distance only at one-time intervals (T1-T2) (*p*-value = 0.006). At 24 hours, the migration distance was highest for 200 µg/ml of BBR-CuONPS nano formulation, which was followed by 100, 50, and 10 µg/ml,

Table 4. Multiple pair wise comparisons of distance of cell migration between study groups at 48 hours.

Treatment group	Drug concentration	Mean difference	p-value
Control	10 µg	-668	<0.001**
	50 µg	-1,527.67	<0.001**
	100 µg	-1,505.34	<0.001**
	200 µg	-1,661.34	<0.001**
10 µg	50 µg	-859.67	<0.001**
	100 µg	-837.34	<0.001**
50 µg	200 µg	-993.34	<0.001**
	100 µg	22.33	0.81
100 µg	200 µg	-133.67	0.11
	200 µg	-156	0.09

Post Hoc Tukey Test; * p -value<0.05 – statistically significant; ** p -value<0.001 – highly statistically significant.

and the control group. This difference in migration distance observed between all the groups was statistically significant (p -value < 0.001). The Post hoc Tukey test was used to carry out multiple pairwise comparisons of the berberine-CuONPs in various concentrations. The results reveal statistically significant differences in migration distances between 10 µg/ml of BBR-CuONPs and all other concentrations such as 50, 100, and 200 µg/ml (p -value < 0.05, respectively). However, there was no significant difference noted in migration distances between 50, 100, and 200 µg/ml BBR-CuONPs, thus indicating their similar effects on migration distance.

Table 4 shows multiple pairwise comparisons of the distance of cell migration between study groups at 48 hours. There was a significant difference in mean migration distance between the control group and BBR-CuONPs at all concentrations such as 10, 50, 100, and 200 µg/ml (p -value < 0.001, respectively). However, there was not much difference in mean migration between 50, 100, and 200 µg of BBR-CuONPs.

Research has shown that the use of berberine at a concentration of 5 mM remarkably reduced cell motility in permanent lung cancer cells (H1299), then compared with glioma (T98G) and prostate cancer (PC3) with the reduction of wound area $74.52\% \pm 12.3\%$, $38.22\% \pm 10.6\%$, and $48.6\% \pm 7.5\%$, was observed after 48 hours, respectively. This highlights that permanent cell lines are more sensitive in anti-migratory activity for berberine compared with primary cell lines of the same condition. Statistical significance was observed in permanent cell lines but not in primary cell lines [84].

In previous research, the cell migration analysis was conducted on the berberine-loaded gold nanoparticles (Au-Col-BB) treated with Bovine Aortic Endothelial Cells (BAEC), non-cancerous cell, and human epidermal growth factor receptor 2 (Her-2) breast cancer cells. It was observed that BAEC cells showed no significant changes in MMP-2 or MMP-9 expression after the drug treatment, suggesting that Au-Col-BB does not affect MMP activity in non-cancerous cells. But in the case of Her-2 cells, MMP-9 expression was lowest

in the Au-Col-BB (10 µg/ml) group at 48 hours. Therefore, MMP-2 expression was significantly reduced in berberine (1 µg/ml) and Au-Col-BB (5, 10 µg/ml) groups, indicating a dose-dependent effect. The cell migration was not inhibited in the BAEC cells, instead, the migration distance was increased at 24 and 48 hours, the Au-Col-BB does not negatively affect the endothelial cell migration, which is important for wound healing. Simultaneously, in the Her-2 cells, it was noted that significant reduction in the cell migration distance after the drug treatments. Finally, complete inhibition was observed in Au-Col-BB treatment for the concentration of 10 µg/ml group at 48 hours [85].

SHELF LIFE AND STABILITY OF BERBERINE-LOADED CUONPS

For long-term storage, lyophilization (freeze-drying) of the copper oxide nanoparticles can be employed. Lyophilization helps preserve the structure and activity of berberine as well as the integrity of the copper oxide nanoparticles during storage [86]. The stabilization of berberine-loaded copper oxide nanoparticles involves the use of solvents and dispersion media for enhancing the solubility, stability, and shelf life. The water is used as a solvent in preserving bioactive compounds. DMSO is commonly used as a solvent for improving the solubility of hydrophobic compounds such as berberine which facilitates the incorporation of nano particles and reduces aggregation risk. E.g., for the preparation of berberine-loaded PEG-PLGA nanoparticles, DMSO is used to dissolve the polymer as well as berberine before nano precipitation takes place leading to stable nanoparticles with enhanced therapeutic efficacy [87].

PBS is used as a dispersion medium that mimics physiological conditions, for the assessment of the stability of nanoparticles in a biological environment. There are limited studies conducted on the shelf life of PBS and it is recognized as a stable medium for the storage of the nano particles. Therefore, copper oxide nanoparticles are well known for their inherent chemical stability, contributing to the overall shelf life of the nano formulation. Incorporating DMSO and PBS in the berberine-loaded CuONPs can significantly enhance their drug efficacy for a longer period.

CHALLENGES AND LIMITATIONS

Though the green synthesis of berberine-embedded copper oxide nano formulation from *Solanum torvum* has potential, some challenges need to be addressed in future research. These include scalability, stability, shelf life, and controlled release of berberine from CuONPs to optimize their therapeutic efficacy. Additionally, the potential toxicity from exceeding safe doses of the formulated drug must be considered. The limitations of using berberine-loaded CuONPs for lung cancer therapy include the need for a deeper understanding of the mechanism of action, such as the molecular signaling pathways (e.g., MAPK/Akt). Furthermore, the lack of targeting ligands for specific delivery to cancer cells and the absence of comprehensive pharmacokinetic and *in vivo* analysis pose significant challenges. Clinical trials are crucial for understanding biocompatibility, biodistribution, and therapeutic efficacy, but these studies are often hindered by interactions

with biological systems and regulatory challenges. Ensuring product quality and managing cost implications for large-scale applications in lung cancer therapy and wound healing are also critical factors. The absence of such studies in this phase of research highlights the need for future investigations to refine these aspects for more effective clinical applications.

CONCLUSION

The implementation for the synthesis of BBR-CuONPs using *S. torvum* has been discovered as a new potential basis for therapeutic use. The characterization studies confirmed the successful nano formulation, ensuring structural integrity and functional stability. The nano-formulation demonstrated significant cytotoxicity against A549 lung cancer cells in a dose-dependent manner, as evidenced by the MTT assay. Beyond, its anticancer activity broadens the pathway to lung cancer treatment emphasizing the multifunctionality and clinical relevance of these formulations. Additionally, the wound healing assay revealed that BBR-CuONPs effectively suppressed cancer cell migration, a critical factor in tumor metastasis, with the highest inhibition observed at 10 µg/ml (24–48 hours). Statistical analysis confirmed the significance of these findings ($p < 0.05$). This study opened new avenues toward research and development of copper oxide berberine nano formulation into smart-formulated drugs for future patient benefits particularly, in oncology and wound healing. The synergistic effect of berberine and CuONPs enhances therapeutic efficacy while maintaining biocompatibility, making both biomedical applications for cancer treatment and wound management. Overall, this study highlights the clinical relevance of BBR-CuONPs, demonstrating their dual functionality in lung cancer treatment and wound healing. The nano-formulation holds great promise for future biomedical applications, and further *in vivo* studies are warranted to establish its therapeutic potential, stability, and safety for clinical use.

AUTHOR CONTRIBUTIONS

All authors made substantial contributions to conception and design, acquisition of data, or analysis and interpretation of data; took part in drafting the article or revising it critically for important intellectual content; agreed to submit to the current journal; gave final approval of the version to be published; and agree to be accountable for all aspects of the work. All the authors are eligible to be an author as per the International Committee of Medical Journal Editors (ICMJE) requirements/guidelines.

FINANCIAL SUPPORT

There is no funding to report.

CONFLICTS OF INTEREST

The authors report no financial or any other conflicts of interest in this work.

ETHICAL APPROVALS

This study does not involve experiments on animals or human subjects.

DATA AVAILABILITY

All data generated and analyzed are included in this research article.

PUBLISHER'S NOTE

This journal remains neutral with regard to jurisdictional claims in published institutional affiliation.

REFERENCES

1. <https://www.iarc.who.int/cancer-type/lung-cancer/>
2. Zhu X, Yu Z, Feng L, Deng L, Fang Z, Liu Z, *et al.* Chitosan-based nanoparticle co-delivery of docetaxel and curcumin ameliorates anti-tumor chemoimmunotherapy in lung cancer. *Carbohydr Polym.* 2021;268:118237.
3. Kozower BD, Lerner JM, Detterbeck FC, Jones DR. Special treatment issues in non-small cell lung cancer: diagnosis and management of lung cancer: American College of chest physicians evidence-based clinical practice guidelines. *Chest.* 2013;143(5 Suppl):e369S–99. doi: <https://doi.org/10.1378/chest.12-2362>
4. Ko EC, Raben D, Formenti SC. The integration of radiotherapy with immunotherapy for the treatment of non-small cell lung cancer. *Clin Cancer Res.* 2018;24(23):5792–806. doi: <https://doi.org/10.1158/1078-0432.CCR-17-3620>
5. Horikoshi S, Serpone N. Introduction to nanoparticles. In: Horikoshi S, Serpone N, editors. *Microwaves in nanoparticle synthesis: fundamentals and applications.* Weinheim, Germany: Wiley-VCH Verlag GmbH and Co. KGaA; 2023. pp. 1–24.
6. Almeida JP, Lin AY, Langsner RJ, Eckels P, Foster AE, Drezek RA. *In vivo* immune cell distribution of gold nanoparticles in naive and tumor-bearing mice. *Small.* 2024;10(5):812–9.
7. Chow EK, Ho D. Cancer nanomedicine: from drug delivery to imaging. *Sci Transl Med.* 2013;5(216):216rv4.
8. Baetke SC, Lammers T, Kiessling F. Applications of nanoparticles for diagnosis and therapy of cancer. *Br J Radiol.* 2015;88:20150207.
9. Markman JL, Rekechenetskiy A, Holler E, Ljubimova JY. Nanomedicine therapeutic approaches to overcome cancer drug resistance. *Adv Drug Deliv Rev.* 2013;65(13–14):1866–79. doi: <https://doi.org/10.1016/j.addr.2013.09.019>
10. Sharma A, Goyal AK, Rath G. Recent advances in metal nanoparticles in cancer therapy. *J Drug Target.* 2019;27(8):709–24. doi: <https://doi.org/10.1080/1061186X.2019.1598611>
11. Danhier F. To exploit the tumor microenvironment: passive and active tumor targeting of nanocarriers for anti-cancer drug delivery. *J Control Release.* 2016;244(Pt A):108–21. doi: <https://doi.org/10.1016/j.jconrel.2016.11.020>
12. In B, Nieva J. Tumor microenvironment acidity enhances the membrane insertion of a pH-sensitive peptide designed to target acidic tissues. *J Mol Biol.* 2015;427(6):1244–58. doi: <https://doi.org/10.1016/j.jmb.2015.02.006>
13. Prabhu RH, Patravale VB, Joshi MD. Polymeric nanoparticles for targeted treatment in oncology: current insights. *Int J Nanomedicine.* 2015;10:1001–18. doi: <https://doi.org/10.2147/IJN.S56932>
14. Bazak R, Houry M, El Achy S, Hussein W, Refaat T. Passive targeting of nanoparticles to cancer: a comprehensive review of the literature. *Mol Clin Oncol.* 2015;2(6):904–8. doi: <https://doi.org/10.3892/mco.2015.670>
15. Wakelee H, Kelly K, Edelman MJ. 50 years of progress in the systemic therapy of non-small cell lung cancer. *Am Soc Clin Oncol Educ Book.* 2014;(34):177–89. doi: https://doi.org/10.14694/EdBook_AM.2014.34.177
16. Nagasaka M, Zaki M, Kim H, Raza SN, Yoo G, Lin HS, *et al.* PD1/PD-L1 inhibition as a potential radiosensitizer in head and neck squamous cell carcinoma: a case report. *J Immunother Cancer.* 2016;4:83. doi: <https://doi.org/10.1186/s40425-016-0187-0>

17. Gurley KE, Moser R, Gu Y, Hasty P, Kemp CJ. DNA-PK suppresses a p53-independent apoptotic response to DNA damage. *EMBO Rep.* 2009;10(1):87–93. doi: <https://doi.org/10.1038/embor.2008.214>
18. Bohlman S, Manfredi JJ. p53-independent effects of Mdm2. *Subcell Biochem.* 2014;85:235–46. doi: https://doi.org/10.1007/978-94-017-9211-0_13
19. Fariq A, Khan T, Yasmin A. Microbial synthesis of nanoparticles and their potential applications in biomedicine. *J Appl Biomed.* 2017;15(4):241–8. doi: <https://doi.org/10.1016/j.jab.2017.03.004>
20. Singh KR, Nayak V, Singh J, Singh AK, Singh RP. Potentialities of bioinspired metal and metal oxide nanoparticles in biomedical sciences. *RSC Adv.* 2021;11(40):24722–46.
21. Mariadoss AV, Saravanakumar K, Sathiyaseelan A, Venkatachalam K, Wang MH. Folic acid functionalized starch encapsulated green synthesized copper oxide nanoparticles for targeted drug delivery in breast cancer therapy. *Int J Biol Macromol.* 2020 Dec 1;164:2073–84.
22. Chavali MS, Nikolova MP. Metal oxide nanoparticles and their applications in nanotechnology. *SN Appl Sci.* 2019;1:607. doi: <https://doi.org/10.1007/s42452-019-0592-3>
23. Mobeen Amanulla M, Bashir S, Jehangir T, *et al.* Copper oxide nanoparticles for photothermal therapy: a study *in vitro*. *J Nanomater.* 2018;2018:7582309.
24. Abraham A, Karthikeyan S, Radhakrishnan R. Antimicrobial potential of copper oxide nanoparticles: a review. *J Biomed Mater Res B Appl Biomater.* 2021;109(5):742–51. doi: <https://doi.org/10.1002/jbm.b.34755>
25. Manimaran A, Rajendran R, Aravinthan A, *et al.* Synthesis and characterization of copper oxide nanoparticles mediated by actinomycetes and their biological applications. *J Nanomater.* 2020;2020:7398291.
26. Bukhari SI, Hamed MM, Al-Agamy MH, Gazwi HS, Radwan HH, Youssif AM. Biosynthesis of copper oxide nanoparticles using streptomyces MHM38 and its biological applications. *J Nanomater.* 2021;2021(1):6693302.
27. Mali, SB. Copper nanoparticles—potential for cancer therapy. *J Maxillofac Oral Surg* 2024. doi: <https://doi.org/10.1007/s12663-024-02374-3>
28. Ezealisiji KM, Obinna-Echem A, Chijioke-Osuji UC. Green synthesis of zinc oxide nanoparticles using *Solanum torvum* (L) leaf extract and evaluation of the toxicological profile of the ZnO nanoparticles–hydrogel composite in Wistar albino rats. *Int Nano Lett.* 2019;9:99–107. doi: <https://doi.org/10.1007/s40089-019-0267-4>
29. D’Incalci M, Steward WP, Gescher AJ. Use of cancer chemopreventive phytochemicals as antineoplastic agents. *Lancet Oncol.* 2005;6(11):899–904.
30. Sarker SD, Nahar L. Chemistry for pharmacy students: general, organic and natural product chemistry. Hoboken, UK: John Wiley and Sons; 2007. pp. 283–359.
31. Amjad M, Iqbal I, Rees D, Iqbal Q, Nawaz A, Ahmed T. Effect of packing materials and different storage regimes on shelf life of green hot pepper fruits. *Acta Hort.* 2010;8:227–34.
32. Chah KF, Muko KN, Oboegbulem SI. Antimicrobial activity of methanolic extract of *Solanum torvum* fruit. *Fitoterapia.* 2000;71(2):187–9.
33. Lee B, Sur B, Shim I, Lee H, Hahm DH. *Phellodendron amurense* and its major alkaloid compound, berberine ameliorates scopolamine-induced neuronal impairment and memory dysfunction in rats. *Korean J Physiol Pharmacol.* 2012;16(2):79–89. doi: <https://doi.org/10.4196/kjpp.2012.16.2.79>
34. Imenshahidi M, Hosseinzadeh H. *Berberis vulgaris* and berberine: an update review. *Phytother Res.* 2016;30(11):1745–64. doi: <https://doi.org/10.1002/ptr.5693>
35. Kumar A. Current knowledge and pharmacological profile of berberine: an update. *Eur J Pharmacol.* 2015;761:288–97. doi: <https://doi.org/10.1016/j.ejphar.2015.05.068>
36. Chen Q, Qin R, Fang Y, Li H. Berberine sensitizes human ovarian cancer cells to cisplatin through miR-93/PTEN/Akt signaling pathway. *Cell Physiol Biochem.* 2015;36(3):956–65. doi: <https://doi.org/10.1159/000430270>
37. Li L, Wang X, Sharvan R, Gao J, Qu S. Berberine could inhibit thyroid carcinoma cells by inducing mitochondrial apoptosis, G0/G1 cell cycle arrest and suppressing migration via PI3K-AKT and MAPK signaling pathways. *Biomed Pharmacother.* 2017;95:1225–31. doi: <https://doi.org/10.1016/j.biopha.2017.09.010>
38. Milata V, Svedova A, Barbierikova Z, Holubkova E, Cipakova I, Cholujova D, *et al.* Synthesis and anticancer activity of novel 9-O-substituted berberine derivatives. *Int J Mol Sci.* 2019;20(9):2169. doi: <https://doi.org/10.3390/ijms20092169>
39. Yang X, Huang N. Berberine induces selective apoptosis through the AMPK-mediated mitochondrial/caspase pathway in hepatocellular carcinoma. *Mol Med Rep.* 2013;8(2):505–10. doi: <https://doi.org/10.3892/mmr.2013.1506>
40. Li W, Jiang T, Gao L, Chen G, Gao Q. Berberine stimulates the intrinsic apoptotic pathway and caspase activation in tumor cells. *J Cell Biochem.* 2018;119(5):4514–21. doi: <https://doi.org/10.1002/jcb.26537>
41. Ma J, Zhao D, Lu H, Huang W, Yu D. Apoptosis Signal-Regulating Kinase 1 (ASK1) activation is involved in silver nanoparticles induced apoptosis of A549 lung cancer cell line. *J Biomed Nanotechnol.* 2017;13(3):349–54. doi: <https://doi.org/10.1166/jbn.2017.2359>
42. Matsuzawa A, Nishitoh H, Tobiume K, Takeda K, Ichijo H. Physiological roles of ASK1-mediated signal transduction in oxidative stress- and endoplasmic reticulum stress-induced apoptosis: advanced findings from ASK1 knockout mice. *Antioxid Redox Signal.* 2002;4(3):415–25. doi: <https://doi.org/10.1089/15230860260196218>
43. Tobiume K, Matsuzawa A, Takahashi T, Nishitoh H, Morita K, Takeda K, *et al.* ASK1 is required for sustained activations of JNK/p38 MAP kinases and apoptosis. *EMBO Rep.* 2001;2(3):222–8. doi: <https://doi.org/10.1093/embo-reports/kve046>
44. Zheng F, Tang Q, Wu J, Zhao S, Liang Z, Li L, *et al.* P38 α MAPK-mediated induction and interaction of FOXO3a and p53 contribute to the inhibited growth and induced apoptosis of human lung adenocarcinoma cells by berberine. *J Exp Clin Cancer Res.* 2014;33:36.
45. Hyun MS, Hur JM, Mun YJ, Kim D, Woo WH. Berberine induces apoptosis in HepG2 cells through an Akt-ASK1-ROS-p38MAPKs-linked cascade. *J Cell Biochem.* 2010;109:329–38.
46. Hur JM, Hyun MS, Lim SY, Lee WY, Kim D. The combination of berberine and irradiation enhances anti-cancer effects via activation of the p38 MAPK pathway and ROS generation in human hepatoma cells. *J Cell Biochem.* 2009;107:955–64.
47. Zhao L, Zhang S, Wang X, Li J, Zhou Y, Hua Y, *et al.* Protective effects of berberine on doxorubicin-induced hepatotoxicity in mice. *Biol Pharm Bull.* 2012;35(5):796–800. doi: <https://doi.org/10.1248/bpb.35.796>
48. Domitrović R, Jakovac H, Blagojević G. Hepatoprotective activity of berberine is mediated by inhibition of TNF- α , COX-2, and iNOS expression in CCl $_4$ -intoxicated mice. *Toxicology.* 2011;280(1–2):33–43. doi: <https://doi.org/10.1016/j.tox.2010.11.004>
49. Chen J, Li W, Cui K, Ji K, Xu S, Xu Y. Artemisitene suppresses tumorigenesis by inducing DNA damage through deregulating c-Myc-topoisomerase pathway. *Oncogene.* 2018;37(37):5079–87. doi: <https://doi.org/10.1038/s41388-018-0331-z>
50. Fan FL, Dart AM. Anti-inflammatory treatment in patients after percutaneous coronary intervention: another potential use for berberine? *Clin Exp Pharmacol Physiol.* 2012;39(5):404–5.
51. Djebbi MA, Elabed A, Bouaziz Z, Sadiki M, Elabed S, Namour P, Jaffrezic-Renault N, Amara AB. Delivery system for berberine chloride based on the nanocarrier ZnAl-layered double hydroxide: physicochemical characterization, release behavior and evaluation of anti-bacterial potential. *Int J Pharm.* 2016;515(1–2):422–30.

52. Barua S, Mitragotri S. Challenges associated with penetration of nanoparticles across cell and tissue barriers: a review of current status and future prospects. *Nano Today*. 2014;9(2):223–43. doi: <https://doi.org/10.1016/j.nantod.2014.04.008>
53. Onoue S, Yamada S, Chan HK. Nanodrugs: pharmacokinetics and safety. *Int J Nanomed*. 2014;9(1):1025–37. doi: <https://doi.org/10.2147/IJN.S38378>
54. Lee, K.J, An JH, Chun JR, Chung KH, Park WY, Shin JS, *et al.* *In vitro* analysis of the anti-cancer activity of mitoxantrone loaded on magnetic nanoparticles. *J Biomed Nanotechnol*. 2013;9:1071–5. doi: <https://doi.org/10.1166/jbn.2013.1530>
55. Ali I, Naqshbandi MF, Husain M. Cell migration and apoptosis in human lung cancer cells by clove (*Syzygium aromaticum*) dried flower buds extract. *J Taibah Univers Sci*. 2019a;13:1163–74. doi: <https://doi.org/10.1080/16583655.2019.1691480>
56. <https://sdgs.un.org/goals>
57. Hsu CY, Pallathadka H, Gupta J, Ma H, Al-Shukri HHK, Kareem AK, *et al.* Berberine and berberine nano formulations in cancer therapy: focusing on lung cancer. *Phytother Res*. 2024;38(8):4336–50. doi: <https://doi.org/10.1002/ptr.8255>
58. Wu C, Dong B, Huang L, Liu Y, Ye G, Li S, *et al.* SPTBN2, a new biomarker of lung adenocarcinoma. *Front Oncol*. 2021;11:754290. <https://doi.org/10.3389/fonc.2021.754290>
59. Hanif A, Ibrahim AH, Ismail S, Al-Rawi SS, Ahmad JN, Hameed M, *et al.* Cytotoxicity against A549 human lung cancer cell line via the mitochondrial membrane potential and nuclear condensation effects of *Nepeta paulesenii* Briq., a perennial herb. *Molecules*. 2023;28(6):2812. Available from: <https://doi.org/10.3390/molecules28062812>
60. Karki R, Kim SB, Kim DW. Magnolol inhibits migration of vascular smooth muscle cells via cytoskeletal remodeling pathway to attenuate neointima formation. *Exp Cell Res*. 2013;319(20):3238–50. doi: <https://doi.org/10.1016/j.yexcr.2013.07.016>
61. Maiuthed A, Chanvorachote P. Cisplatin at sub-toxic levels mediates integrin switch in lung cancer cells. *Anticancer Res*. 2014;34(12):7111–8.
62. Alao II, Oyekunle IP, Iwuozor KO, Emenike EC. Green synthesis of copper nanoparticles and investigation of its antimicrobial properties. *Adv J Chem. B*. 2022;4(1):39–52. <https://doi.org/10.22034/ajcb>
63. Tavade S, Patil K, Kurangi B, Suryawanshi S. Development and validation of UV-spectrophotometric method for estimation of berberine hydrochloride in marketed formulation and poly lactic co-glycolic acid nanoparticles. *Indian J Pharm Educ Res*. 2022;56(3):873–8. doi: <https://doi.org/10.5530/ijper.56.3.120>
64. Nasrollahzadeh M, Maham M, Rostami-Vartooni A, Bagherzadeh M, Sajadi SM. Barberry fruit extract assisted in situ green synthesis of Cu nanoparticles supported on a reduced graphene oxide–Fe³O₄ nanocomposite as a magnetically separable and reusable catalyst for the O-arylation of phenols with aryl halides under ligand-free conditions. *RSC Adv*. 2015;5(95):75909–18. doi: <https://doi.org/10.1039/c5ra10037b>
65. Younis FA, Saleh SR, El-Rahman SSA, Newairy AA, El-Demellawy MA, Ghareeb DA. Preparation, physicochemical characterization, and bioactivity evaluation of berberine-entrapped albumin nanoparticles. *Sci Rep*. 2022;12:17431. doi: <https://doi.org/10.1038/s41598-022-21568-8>
66. Aljedaani RO, Kosa SA, Abdel Salam M. Ecofriendly green synthesis of copper (II) oxide nanoparticles using *Corchorus olitorius* leaves (Molokhaia) extract and their application for the environmental remediation of direct violet dye via advanced oxidation process. *Molecules*. 2023;28(1):16. doi: <https://doi.org/10.3390/molecules28010016>
67. Lakhotiya G, Bajaj S, Nayak AK, Pradhan D, Tekade P, Rana A. Enhanced catalytic activity without the use of an external light source using microwave-synthesized CuO nanopetals. *Beilstein J Nanotechnol*. 2017;8:1167–73. doi: <https://doi.org/10.3762/bjnano.8.118>
68. Rajivgandhi GN, Ramachandran G, Kannan MR, Velanganni AAJ, Siddiqi MZ, Alharbi NS, *et al.* Photocatalytic degradation and anti-cancer activity of biologically synthesized Ag NPs for inhibiting MCF-7 breast cancer cells. *J Photochem Photobiol B*. 2020;203:111748.
69. Tian Y, Zhao L, Wang Y, Zhang H, Xu D, Zhao X, *et al.* Berberine inhibits androgen synthesis by interaction with aldo-keto reductase 1C3 in 22Rv1 prostate cancer cells. *Asian J Androl*. 2016;18(6):607–12. doi: <https://doi.org/10.4103/1008-682X.169997>
70. Wang J, Qi Q, Feng Z, Zhang X, Huang B, Chen A, *et al.* Berberine induces autophagy in glioblastoma by targeting the AMPK/mTOR/ULK1 pathway. *Oncotarget*. 2016;7(43):66944–58. doi: <https://doi.org/10.18632/oncotarget.11396>
71. Eo HJ, Park JH, Park GH, Lee MH, Lee JR, Kim MK, *et al.* Berberine-induced cell cycle arrest and apoptosis in human cancer cells. *J Med Food*. 2015;18(1):37–45. doi: <https://doi.org/10.1089/jmf.2014.0085>
72. Mirhadi E, Rezaee M, Malaekheh-Nikouei B. Nano strategies for berberine delivery, a natural alkaloid of *Berberis*. *Biomed Pharmacother*. 2018;104:465–73. doi: <https://doi.org/10.1016/j.biopha.2018.05.067>
73. Siddiqui MA, Alhadlaq HA, Ahmad J, Al-Khedhairi AA, Musarrat J, Ahamed M. Copper oxide nanoparticles induced mitochondria mediated apoptosis in human hepatocarcinoma cells. *PLoS One*. 2013 Aug 5;8(8):e69534. doi: <https://doi.org/10.1371/journal.pone.0069534>
74. Da Violante G, Zerrouk N, Richard I, Provot G, Chaumeil JC, Arnaud P. Evaluation of the cytotoxicity effect of dimethyl sulfoxide (DMSO) on Caco2/TC7 colon tumor cell cultures. *Biol Pharm Bull*. 2002 Dec;25(12):1600–3. doi: <https://doi.org/10.1248/bpb.25.1600>. PMID: 12499647
75. Zhou W, Zi L, Cen Y, You C, Tian M. Copper sulfide nanoparticles-incorporated hyaluronic acid injectable hydrogel with enhanced angiogenesis to promote wound healing. *Front Bioeng Biotechnol*. 2020;8:417.
76. Alarifi S, Ali D, Verma A, Alakhtani S, Ali BA. Cytotoxicity and genotoxicity of copper oxide nanoparticles in human skin keratinocytes cells. *Int J Toxicol*. 2016;32:296–307.
77. Wu Z, Zhang W, Kang YJ. Copper affects the binding of HIF-1alpha to the critical motifs of its target genes. *Metallomics*. 2019;11:429–38.
78. Brillet G, Deray G, Jacquiau C, Mignot L, Bunker D, Meillet D, *et al.* Long-term renal effect of cisplatin in man. *Am J Nephrol*. 1994 Oct 28;14(2):81–4.
79. Kraatz HB, Metzler-Nolte N, editors. *Bioinorganic chemistry*. Weinheim, Germany: Wiley-VCH; 2006. p. 443.
80. Bhanumathi R, Vimala K, Shanthi K, Thangaraj R, Kannan S. Bioformulation of silver nanoparticles as berberine carrier cum anticancer agent against breast cancer. *N J Chem*. 2017;41:14466–77. doi: <https://doi.org/10.1039/C7NJ02531A>
81. Taebpour M, Arasteh F, Akhlaghi M, Haghrosadat BF, Oroojalian F, Tofighi D. Fabrication and characterization of PLGA polymeric nanoparticles containing Berberine and its cytotoxicity on breast cancer cell (MCF-7). *Nanomed Res J*. 2021;6(4):259–68. doi: <https://doi.org/10.22034/nmrj.2021.04.009>
82. Bhattacharya T, Maishu SP, Akter R, Rahman MH, Akhtar MF, Saleem A, *et al.* A review on natural sources derived protein nanoparticles as anticancer agents. *Curr Top Med Chem*. 2021;21:1014–26.
83. Piret JP, Jacques D, Audinot JN, Mejia J, Boilan E, Noël F, *et al.* Copper (II) oxide nanoparticles penetrate into HepG2 cells, exert cytotoxicity via oxidative stress and induce pro-inflammatory response. *Nanoscale*. 2012;4:7168–84. doi: <https://doi.org/10.1039/c2nr31804g>

84. Timofeeva SV, Kit OI, Filippova SY, Sitkovskaya AO, Mezheva IV, Gnennaya NV, *et al.* Effect of berberine on cancer cell motility in glioma, lung cancer, and prostate cancer cell cultures. *J Clin Oncol.* 2022;40:e15079.
85. Chiu CF, Fu RH, Hsu SH, Yu YH, Yang SF, Tsao TCY, *et al.* Delivery capacity and anticancer ability of the berberine-loaded gold nanoparticles to promote the apoptosis effect in breast cancer. *Cancers.* 2021;13(21):5317. doi: [https://doi.org/ 10.3390/cancers13215317](https://doi.org/10.3390/cancers13215317)
86. Mishra R, Aher A. Lipid-based berberine loaded lyophilized nano micelles with enhanced antioxidant effect: design and characterization. *J Appl Pharm Sci.* 2024;14(06):126–34. doi: <https://doi.org/10.7324/JAPS.2024.154408.K>
87. Shen F, Zheng YS, Dong L, Cao Z, Cao J. Enhanced tumor suppression in colorectal cancer via berberine-loaded PEG-PLGA nanoparticles. *Front Pharmacol.* 2024 Nov 1;15:1500731. Available from: <https://doi.org/10.3389/fphar.2024.1500731>

How to cite this article:

Sakthivel MB, Devi NP, Munusamy T, Devarajan N, Amritkumar P, Malchi S, Kumar KN, Karunanidhi K. Berberine-enriched copper oxide nano formulation synthesized using *Solanum torvum*: A strategic advancement in lung cancer therapy and wound healing. *J Appl Pharm Sci.* 2025;15(06):096–114. DOI: 10.7324/JAPS.2025.237203